SYSTEM FOR AIDING COIL EMBOLIZATION PLANNING
IN INTRACRANIAL ANEURYSM

Mr. Wiwat Owasirikul

A Dissertation Submitted in Partial Fulfillment of Requirements for the

Degree of Doctor of Philosophy Program in Biomedical Engineering

Interdisciplinary Program Faculty of Engineering

Chulalongkorn University

Academic Year 2011

Copyright of Chulalongkorn University

ระบบช่วยวางแผนการรักษาโรคหลอดเลือดสมองโป่งพองด้วยขดลวดอุดกั้น

นายวิวัฒน์ โอวศิริกุล

Thesis Title   System for Aiding Coil Embolization Planning in Intracranial
                    Aneurysm
By   Mr. Wiwat Owasirikul
Field of Study   Biomedical Engineering
Thesis advisor   Assistant Professor Supatana Auethavekiat, Ph.D.
Thesis co-advisor   Assistant Professor Jaturon Tantivatana, M.D.

_____

        Accepted by the Faculty Engineering, Chulalongkorn University in Partial
Fulfillment of the Requirements for the Doctoral Degree

        …………………………………Dean of the Faculty of Engineering
        (Associate Professor Boonsom Lerdhirunwong, Ph.D.)

THESIS COMMITTEE
        …………………………………Chairman
        (Associate Professor Mana Sriyudthsak, Ph.D.)

        …………………………………Thesis advisor
        (Assistant Professor Supatana Auethavekiat, Ph.D.)

        …………………………………Thesis co-advisor
        (Assistant Professor Jaturon Tantivatana, M.D.)

        …………………………………Examiner
        (Associate Professor Kiat Arjhansiri, M.D.)

        …………………………………Examiner
        (Assistant Professor Charnchai Pluempitiwiriyawej, Ph.D.)

        …………………………………External examiner
        (Assistant Professor Sukanya Phongsuphap, Ph.D.)

วิวัฒน์ โอวศิริกุล : ระบบช่วยวางแผนการรักษาโรคหลอดเลือดสมองโป่งพองด้วยขดลวด
อุดกั้น. (SYSTEM FOR AIDING COIL EMBOLIZATION PLANNING IN
INTRACRANIAL ANEURYSM) อ.ที่ปรึกษาวิทยานิพนธ์หลัก: ผศ.ดร.สุพัฒนา เอื้อ
ทวีเกียรติ, อ.ที่ปรึกษาวิทยานิพนธ์ร่วม: ผศ.นพ. จาตุรนต์ ตันติวัฒนะ, 54 หน้า.

ความสำเร็จในการรักษาโรคหลอดเลือดสมองโป่งพองด้วยขดลวดอุดกั้นขึ้นอยู่กับขนาด
ขดลวดอุดกั้นที่ใส่เข้าไป แต่เมื่อการกระจายตัวของขดลวดอุดกั้นที่อยู่ภายในหลอดเลือดสมองโป่ง
พองมีความยากต่อการทำนายจึงทำให้รังสีแพทย์นิยมเลือกใช้ขนาดขดลวดอุดกั้น(โดยเลือกจาก
ขนาดเส้นผ่าศูนย์กลางรูปร่างและความยาว) จากประสบการณ์เป็นสำคัญ จากปัญหาดังกล่าวจึง
ได้ออกแบบระบบเพื่อศึกษารูปแบบการเลือกขนาดขดลวดอุดกั้น 3 เส้นแรกของรังสีแพทย์ แต่ทว่า
ได้ทำการศึกษาเฉพาะขนาดเส้นผ่าศูนย์กลางรูปร่างเท่านั้น เนื่องจากบ่อยครั้งรังสีแพทย์เลือกใช้
ความยาวขดลวดอุดกั้นที่มากที่สุดในการรักษา ในการศึกษาครั้งนี้ได้ออกแบบระบบจาก 87 ข้อมูล
ทั้งสิ้นสามระบบ ได้แก่ ระบบทำนายขนาดแบบถดถอย ระบบคัดแยกขนาด และระบบผสม
ระหว่างสองระบบข้างต้น โดยวัดประสิทธิภาพในการทำนายขนาดเส้นผ่าศูนย์กลางรูปร่างด้วยวิธี
ดึงข้อมูลออกเพียงหนึ่งตัวแบบหมุนวน ผลที่ได้บ่งชี้ว่าระบบทำนายขนาดแบบถดถอยสามารถ
เลือกขนาดขดลวดอุดกั้นเส้นที่หนึ่งได้ และระบบผสมที่เกิดจากตัวคัดแยกขนาดแบบ Bagging กับ
ระบบทำนายขนาดแบบถดถอยสามารถเลือกขนาดขดลวดอุดกั้นเส้นที่สองและสามได้ แต่ทว่า
ระบบคัดแยกขนาดแบบ Bagging ต้องใช้จำนวนข้อมูลในการฝึกฝนระบบไม่ต่ำกว่า 10 ข้อมูล จึง
จะสามารถเลือกขนาดให้ผิดพลาดอยู่ในช่วงหนึ่งเบอร์ของขนาดขดลวดอุดกั้นได้ ระบบดังกล่าว
นำมาสร้างระบบตอบสนองเพื่อความสะดวกในการใช้งานจริงทางเวชปฏิบัติ โดยมีผลยืนยัน
ประสิทธิภาพในการทำนายขนาดขดลวดอุดกั้นและความปลอดภัยในการเลือกใช้ขดลวดอุดกั้น
ตามระบบตอบสนองด้วยการทดลองในหลอดเลือดสมองโป่งพองจำลอง

สาขาวิชา......วิศวกรรมชีวเวช.......   ลายมือชื่อนิสิต...

ปีการศึกษา..........2554...............   ลายมือชื่อ อ.ที่ปรึกษาวิทยานิพนธ์หลัก............................

                        ลายมือชื่อ อ.ที่ปรึกษาวิทยานิพนธ์ร่วม............................

518 78201 21: MAJOR BIOMEDICAL ENGINEERING

KEYWORDS : INTRACRANIAL ANEURYSM/ EMBOLIZED COIL/ PLANNING AIDING SYSTEM

WIWAT OWASIRIKUL: SYSTEM FOR AIDING COIL EMBOLIZATION PLANNING IN INTRACRANIAL ANEURYSM. ADVISOR: ASST. PROF. SUPATANA AUETHAVEKIAT, Ph.D., CO-ADVISOR: ASST. PROF. JATURON TANTIVATANA, M.D., 54 pp.

The success of the intracranial aneurysm treatment by coil embolization depends on the size of coils inserted into an aneurysm. Since it is difficult to predict how coils distribute inside the aneurysm, radiologists often select coil dimension (the shape diameter (SD) and the length) by experience. The aim of this study is to design a system to model the selection pattern of the radiologist for the first three coils inserted into the aneurysm. Only the SD selection is modeled, since the radiologist often selects the longest available coils. Regression systems (RS), classification systems (CS) and hybrid systems (HS) were investigated. 87 training data were used to create the model. The efficiency of the three systems was measured using the leave-one-out cross validation (LOOCV) method. The LOOCV results indicates that the RS should be used for the first coil selection and the HS consisting of Bagging classifier and the RS should be used for the selection of the second and the third coils. According to the experiment on 13 validating dataset, the SD should be selected by CS if it had at least 10 training data; otherwise, it should be selected by RS. In most cases, the predicted SD was within 1mm of the SD used in the actual treatment. In one aneurysm, different radiologists may use coil with different SD, so the interactive system is implemented such that users can select SD within 1mm of the predicted SD. In vitro experiment was performed to ensure the effectiveness and the safety of the proposed interactive system.

Field of Study : <u>Biomedical Engineering</u>   Student's Signature..................................

Academic Year : ....2011................   Advisor's Signature..................................

Co-advisor's Signature.............................

ACKNOWLEDGEMENTS

The excellent successful of this dissertation depends on the contribution of many people. Especially, I wish to first express gratitude and deepest appreciation to my supervisor: Assistant Professor Dr. Supatana Auethavekiat and Assistant Professor Jaturon Tantivatana, M.D., for their supervision, guidance, encouragement and invaluable advice during my whole doctoral study. I would like to greatly thank staffs at interventional radiology, division of Radiology, King Chulalongkorn Memorial Hospital, Bangkok for their kind contribution and suggestion to this work. Especially, Miss Romrangsri Wongsung and ev3 company for their kind support of embolized coil on in vitro experiment.

I would like to express my deep gratitude and appreciation to my thesis defense committees [Associate Professor Dr. Mana Sriyadthsak (chairman), Associate Professor Kiat Arjhansiri, M.D. (examiner), Assistant Professor Dr. Charnchai Pluempitiwiriyawej (examiner) and Assistant Professor Dr. Sukanya Phongsuphap (external examiner)] for their suggestion and recommendation of thesis detail in order to improve its quality.

I would like to thank the 90th Anniversary of Chulalongkorn University Fund (Ratchadaphiseksomphot Endowment Fund) for the research grant to this study. I also thank Office of the Higher Education Commission (OHEC) for the grant under the University Development Commission (UDC) fellowship in the Ph.D. Program Thai Doctoral degree. Moreover, I express my gratitude to all lecturers, staffs and friends in Biomedical Engineering Program, Chulalongkorn University, for their unlimited teaching throughout whole study, their cheerfulness and their kind supports.

Finally, I am grateful to my family for their care and love. I dedicate this thesis to my father, my mother and all teachers who have taught me since my childhood.

LIST OF TABLES

LIST OF FIGURES

Figure **Page**

Figure **Page**

LIST OF ABBREVIATIONS

2D	two dimensions
ACoA	anterior communicating artery
AdaBoost	adaptive boosting
Bagging	bootstrap aggregating
cm	centimeter
CEV	coil embolization volume
CFD	computational fluid dynamic
CS	classification system
CT	computed tomography
CTA	computed tomography angiography
DSA	digital subtraction angiogram
GDC	guglielmi detachable coil
HS	hybrid system
IAV	intracranial aneurysm volume
ICA	internal carotid artery
L	length of embolized coil
LOOCV	leave-one-out-cross-validation
mm	millimeter
M	the length of a major axis
MRA	magnetic resonance angiography
N	the length of a minor axis
N/A	non-applicable
OD	outer diameter
PCoA	posterior communicating artery
RD	remaining diameter
RPR	radiographic packing rate
RS	regression system
RV	remaining volume
SCA	superior cerebella artery
SD	shape diameter

| SVM | support vector machine |
| VPR | volumetric packing rate |

CONTENTS

CHAPTER I

INTRODUCTION

1.1 RATIONALE

An aneurysm is an abnormal localized dilation of a blood vessel. Due to hemodynamic properties, the aneurysm mostly occurs in an artery. Intracranial aneurysm is one of the risk factors for the prevalence of modality and mortality rate in adults. It was reported that the mortality rate from subarachnoid hemorrhage because of its rupture was about 50% [1]. One of the popular treatments for intracranial aneurysm is the coil embolization, proposed by Guglielmi in 1991 [2]. In this treatment, coils are packed into the aneurysm to occlude the blood from flowing into aneurysm sac. Coil embolization is minimally invasive and causes less complication than the classical surgery treatment [3]. However, if the size of embolized coils is not properly selected, it has the higher probability of the aneurysm recurrence [4].

When a coil is inserted into an aneurysm, its movement is governed by the complex mechanics of the blood flow, the property of the coil and the movement of a catheter. It is difficult to select the appropriate dimension of the coil for the given aneurysm; thus, in clinical practice, the coil is selected based on neurointerventional radiologists' experience which is the subjective decision. One of the major challenges in the coil's size evaluation is the interpretation for 3D vascular structures in a 2D fluoroscopic and arteriographic image. Though 3D imaging provides the accurate aneurysm shape, it is available in only a few cases whose aneurysm has a complex shape and requires a customized approach.

Since in clinical practices, the coil selection is the subjective decision. It is well known that the decision support system can effectively model the selection pattern of a given human sample; therefore, in this research, the system is used to model the selection pattern of the radiologist expert. The model of the system is derived from his/her previous successful treatments.

1.2 Research Objectives

1.To construct a decision support system for selecting the suitable embolized coil in intracranial aneurysm treatment.

2. To evaluate an effectiveness of the proposed system by an in vitro experiment.

1.3 Scope of research

In this research, the system for the selection of the first three embolized coils inserted into the patient is proposed. Its input is the information available from a 2D angiographic projection image. The inclusion criteria of the intracranial aneurysm considered in this research are as follows:

(1) The aneurysm with the saccular shape,

(2) The length of the dome size (major axis length) not exceeding 15 mm,

(3) The ratio of the major versus minor axes between 0.5-2.

1.4 Acceptance threshold

The prediction (selection) error of 1 mm for the shape diameter (SD) of an embolized coil is acceptable.

1.5 Research limitation

1. The number of retrospective data

2. The high cost of embolized coils leading to the limit number of the in vitro experiment.

1.6 Definition

(1) Embolized coil: an endovascular device controllable occlusive soft coil for intracranial aneurysm treatment.

(2) Decision support system: interactive and computer-based systems that aid users in judgment and choice activities [5].

(3) Intracranial aneurysm: an abnormal, localized dilatation of a cerebral artery [6].

(4) Major axis length: the maximum length measured from aneurysm's neck to aneurysm's dome. In most cases, it is measured on a biplane fluoroscopic image.

(5) Minor axis length: the maximum length of aneurysm's width. Typically, it is measured perpendicularly to the major axis on a biplane fluoroscopic image.

1.7 Expected benefit

The system can be beneficial in helping physicians select the appropriate size of an embolized coil. Furthermore, the system in an in vitro experiment can later be used as the practicing tool for radiologists on the treatment by the coil embolization.

1.8 Procedures for research

Figure 1.1 shows the procedure for this study. It is divided into two main parts: the decision support system and the model for in vitro study. Retrospective data is used to construct and evaluate the system. Aneurysm model made from silicone is used in the in vitro study to evaluate the efficiency and the safety of the system. Due to the high cost of the embolized coil, only two silicone models were used in this study.
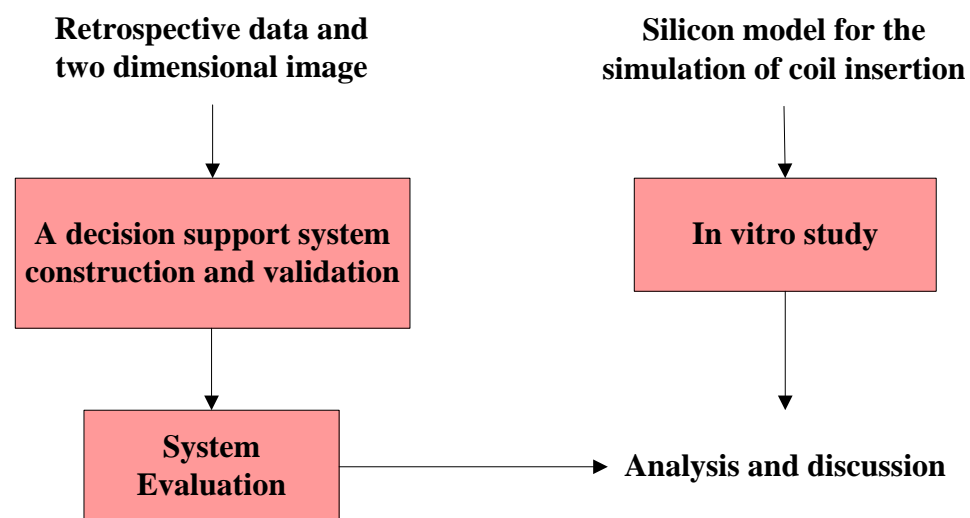
Figure 1.1 Research procedure

CHAPTER II

THEORIES AND LITERATURE REVIEWS

2.1 Principles and Theories

2.1.1 Intracranial aneurysm

An intracranial aneurysm is defined as an abnormal, outward swelling (bubbling) of the wall of the cerebral artery due to the weakness in the wall at that particular site [7]. Approximately 90% of the intracranial aneurysm has the saccular shape [8] as shown in Figure 2.1(a). Other shapes are fusiform (Figure 2.1(b)) and dissecting shape (Figure 2.1(c)). In this research, only saccular aneurysms are considered. Most of intracranial aneurysms are founded surrounding the circle of Willis as shown in Figure 2.2. The site with the highest probability of occurrence is the anterior communicating artery (approximately 30%). The sizes of the intracranial aneurysm, reported in millimeters (mm), are categorized into four groups: small (less than 5mm), medium (between 5-15mm), large (between 15-25mm), and giant aneurysms (more than 25mm). Most aneurysms founded in Thai people are of the small and the medium types.

(a)　　　　(b)　　　　(c)
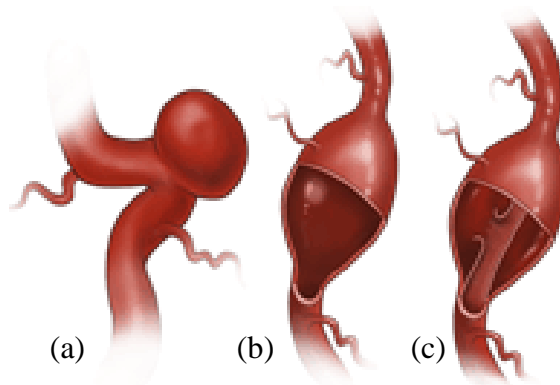
Figure 2.1 Various aneurysm shapes [9]; (a) Saccular or berry shape (most common), (b) Fusiform shape and (c) Dissecting shape.

Anterior communicating
artery (30% to 35%)

Internal carotid
artery/posterior
communicating
artery (30% to 35%)

Basilar
apex
(5%)

Middle
cerebral
artery (20%)

Vertebrobasilar
junction (2%)

Superior
cerebellar
artery (3%)

Posterior inferior
cerebellar artery (3%)
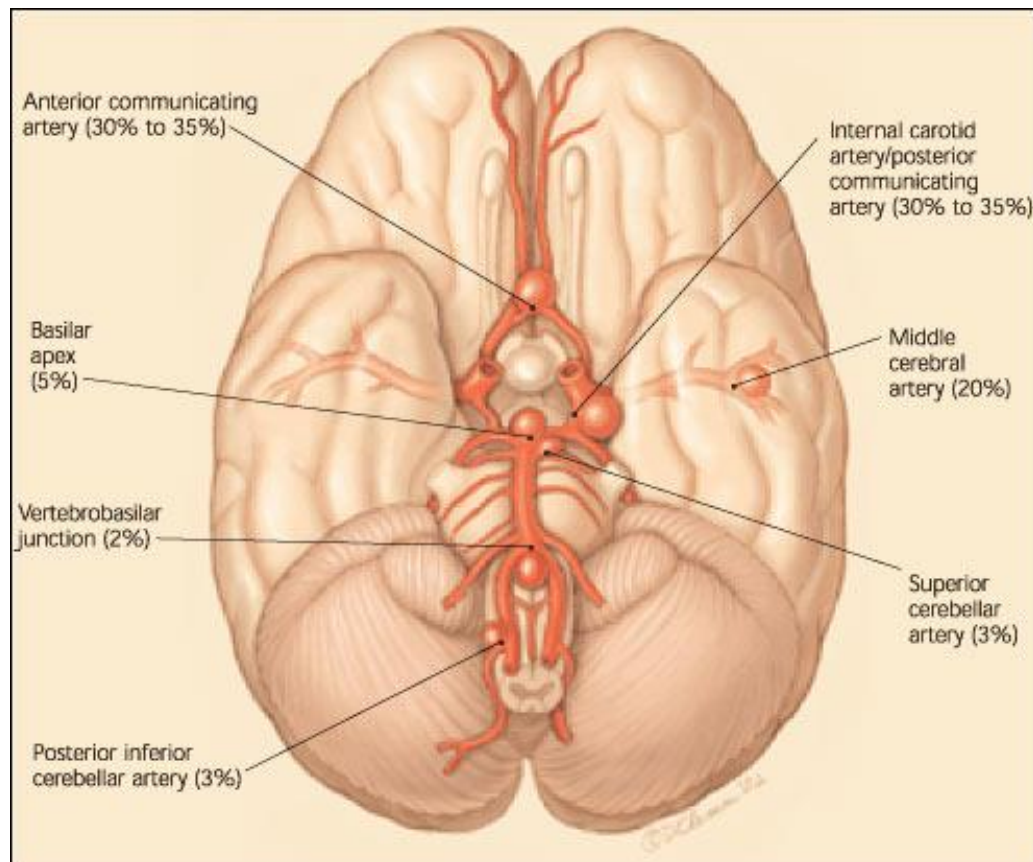
Figure 2.2 The sites of intracranial saccular aneurysms and its probability of occurrence [10]

Three methods of choice to identify or reveal an intracranial aneurysm and to delineate the size and the morphologic features are CT angiography (CTA) after a venous injection, magnetic resonance angiography (MRA), and angiography by direct intra-arterial catheterization (catheter angiography). There are two options for treating intracranial aneurysm: craniotomy with clip ligation (clipping) (Figure 2.3(a)) and endovascular occlusion with the use of detachable coils (coil embolization) (Figure 2.3(b)). The treatment by clipping is performed by a neurosurgeon while the treatment by coil embolization is done by an interventional neuroradiologist. In the coil embolization, a microcatheter is advanced into the aneurysm, then detachable coils of various sizes and shapes are deployed to decrease the amount of blood or to stop blood from filling the aneurysm. The coil embolization has been increasingly used as the treatment for the small aneurysm, since it is less physiologically stressful than the clipping [11-13]. However, it has been indicated in some medical reports that 63%

and 25% of the coil embolization failed in the treatment of the giant and wide-neck aneurysm, respectively [14]. Moreover, if the sizes of the embolized coils are not properly selected, it has the higher probability of the aneurysm recurrence [4].
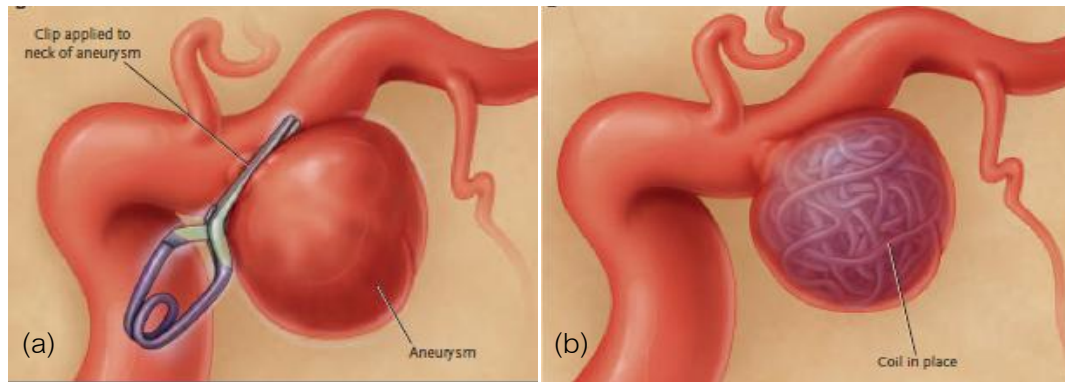
Figure 2.3 Intracranial aneurysm treatment: (a) microsurgical clipping (classical treatment) and (b) endovascular coil embolization (alternative treatment) [15]

2.1.2 Coil embolization

The treatment by endovascular coil embolization has grown substantially and accepted widely as the treatment for intracranial aneurysms. This technique was first proposed by Guglielmi in 1991. Because the embolized coil is an endovascular device, biocompatibility is the most important factor to be considered. The biocompatible coil is primarily composed of an inert material, so that the systemic host response is minimal. Metal alloy is the main composition of the coil, because of its approved record for patient safety. The physical structure of the embolized coil consists of three transformation series from a primary ($1°$) to a secondary ($2°$) to a tertiary ($3°$) structures [16] (Figure 2.4). The diameter of the $1°$ structure is fabricated in the range of 0.00175 - 0.003 inch. The $1°$ structure is wound around a mandrel to produce the $2°$ structure of the coil. The diameter of the $2°$ structure is defined as the outer diameter (OD). Typical OD is between 0.01 and 0.015 inch. The length of the embolized coil (L) is defined as the length of the $2°$ structure. The $2°$ structure can be shaped into the $3°$ structure either in a helical shape or a spherical shape, The $3°$ structure is described by the shape diameter (SD). Two parameters serving as the central factors in package labeling and coil selection are SD and L. In clinical practice,

the physician often selects first the SD and then chooses L from the available L of the selected SD.
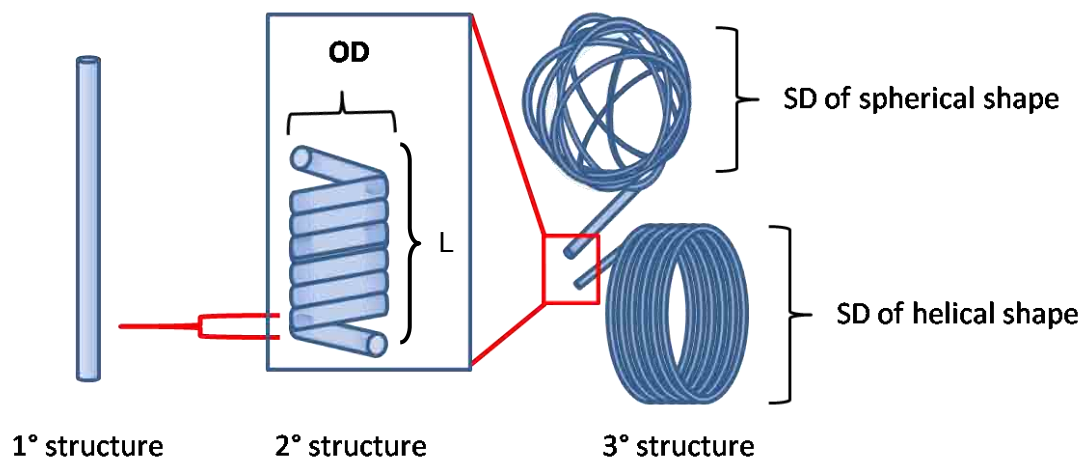
Figure 2.4 Three structures of an embolized coil. Very small wire of the 1° structure is wound around a mandrel to form a helical spring shape of the 2° structure. The 2° structure is shaped into the 3° structure either as a helix or a sphere.

2.1.3 Decision support system

The selection of an embolized coil is a subjective decision, and depends on the experience and skill of an interventional neuroradiologist. Within this background, a decision support system is introduced as an unbiased and objective supporter for decision-making. In this study, a regression system (RS) and a classification system (CS) were investigated. The combination of RS and CS was also investigated.

2.1.3.1 Regression system (RS). RS is a simple technique for predicting numerical output based on a mathematical function. Several types of mathematical functions (E.g. linear, polynomial, exponential, etc.) can be used to predict the unknown output. The training data are used to estimate the parameters of the predicting function. In coil selection problem, the function is used to map between the features available in the aneurysm's image (input) to the size of an embolized coil (output).

2.1.3.2 Classification system (CS). Machine learning is one of the popular methods for classification techniques. It models the pattern according to the training data set. There are two types of machine learning: supervised and unsupervised

learning. In the supervised learning, it is required that the training data set consists of the inputs and their corresponding outputs (label). In the unsupervised learning, the outputs of the training data set are not required. In this research, the supervised machined learning was used for CS construction.

Supervised classification is one of the tasks most frequently carried out by the so-called Intelligent System. Typical characteristics of popular supervised learning algorithms are reported in [17] and some of them are shown in Table 2.1. The table is used as a guide for algorithm selection. The high predicting accuracy is archived by Bagging, Boosting, and Support Vector Machine (SVM). SVM was found to be the good classification in many researches [18-20]. Bagging and Boosting techniques are the examples of ensemble techniques and provide high prediction accuracy, when the size of data set is small [21]. These three classification algorithms are reviewed in this section.

Table 2.1 Characteristics of classification by supervised machine learning. [22]

Algorithm	Predicting accuracy	Fitting speed	Prediction speed	Memory usage
Decision tree	Low	Fast	Fast	Low
Boosting	High	Medium	Medium	Medium
Bagging	High	Slow	Slow	High
SVM	High	Medium	*	*
Naive Bayes	Low	**	**	**
Nearest Neighbor	***	Fast	Medium	High

*SVM provides a good speed and requires low memory usage when there are few support vectors, but is a poor classifier when there are many support vectors.

**Naive Bayes provides a good speed and requires low memory usage for simple distributions, but is a poor classifier for kernel distributions and large data sets.

***Nearest Neighbor usually has good predictions in low dimensions, but can have poor predictions in high dimensions.

2.1.3.2.1 Support vector machines (SVM)

The SVM was first introduced by Vapnik in 1995 under the concept of linear optimal hyperplane construction [23-24]. Its objective is to find the hyperplane that maximizes the space between classes. Nonlinear problems are converted to linear problems by the mapping of inputs. Figure 2.5 shows one such example. The original classifier requires a non-linear circular plane to separate inputs into two classes; however, when the input is mapped to the domain on the right, the linear plane can be used. The mapping in SVM is not strictly defined. Examples of mapping functions, as known as kernel functions (κ) [25], are as follows.
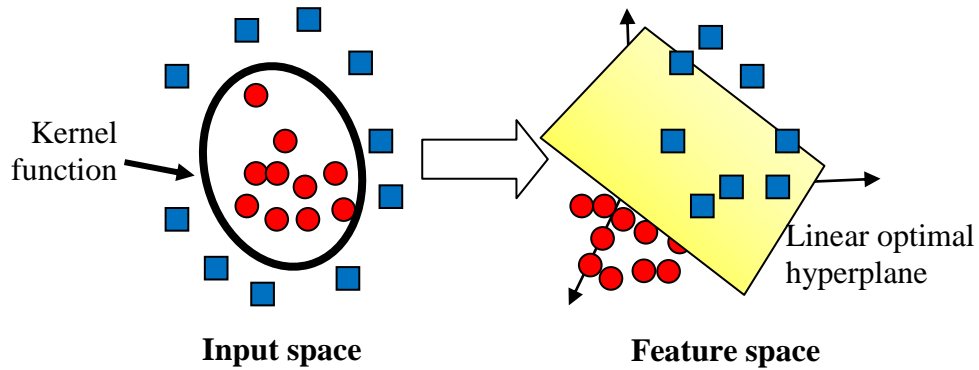
Figure 2.5 illustration of the mapping process from input space to feature space

Gaussian radial basis function $\kappa(\mathbf{X}, \mathbf{Y}) = \exp\left(-\dfrac{\|\mathbf{X}-\mathbf{Y}\|^2}{2\sigma^2}\right),$ (2.1)

where $\mathbf{X}$ is the column vector representing the input features;

$\mathbf{Y}$ is the column vector representing the support vector;

σ is the standard deviation (predefined).

Sigmoid function $\kappa(\mathbf{X}, \mathbf{Y}) = \tanh\left(2\mathbf{X}^\mathrm{T}\mathbf{Y}+1\right),$ (2.2)

where $\mathbf{X}^\mathrm{T}$ is the transpose of $\mathbf{X}$.

Linear function $\kappa(\mathbf{X}, \mathbf{Y}) = \mathbf{X}^\mathrm{T}\mathbf{Y}$ (2.3)

Polynomial function $\kappa(\mathbf{X}, \mathbf{Y}) = \left(\mathbf{X}^\mathrm{T}\mathbf{Y}+1\right)^\mathrm{n},$ (2.4)

where n is the polynomial order (2, 3…).

The efficiency of SVM depends on how well the kernel function suits the problem. In this study, the size of the training dataset is small; thus, the linear kernel function is used [26].
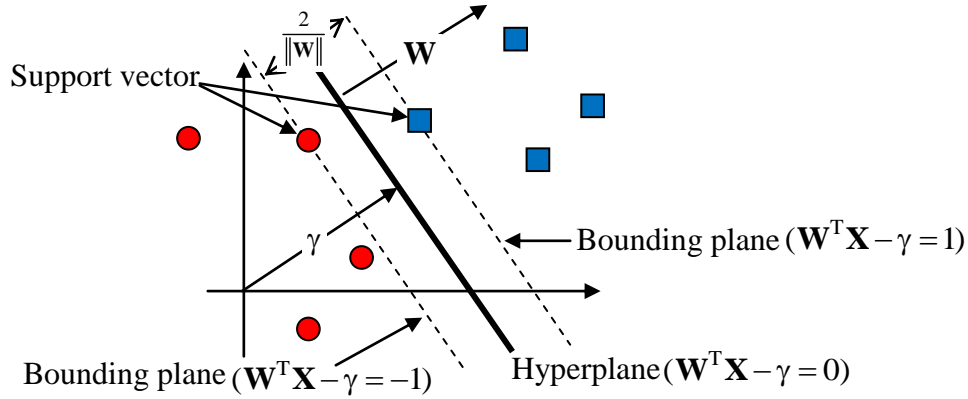
Figure 2.6 Illustration of the hyperplane in SVM.

Figure 2.6 illustrates the concept of SVM for 2-class classifier (the square (1) and the circular classes (-1)). For ease of description, it is assumed that data have been mapped to the linear domain. A support vector is defined as the training datum at the bounding plane. The exact boundary between the two classes is unknown; therefore, if the input is mapped into the space between these two boundary planes, its class will not be well defined. The general rule is to classify the input to the class whose bounding plane is the nearest. The hyperplane to separate the two classes, therefore, locates at the middle of the two bounding planes. In order to reduce the classification error, the distance between the bounding planes (margin) is maximized, so that only few inputs will be mapped to the wrong side of the hyperplane. Define the equation of the hyperplane as $\mathbf{W}^{\mathrm{T}}\mathbf{X} - \gamma = 0$, where $\mathbf{W}$ is the normal vector of the hyperplane and γ is the scalar intersection value and the equation of the two bounding planes are $\mathbf{W}^{\mathrm{T}}\mathbf{X} - \gamma = \pm\mathbf{1}$. The margin between the two bounding planes is $\frac{2}{\|\mathbf{W}\|}$, where $\|\mathbf{W}\|$ is the L2 norm of $\mathbf{W}$. The training phase of the SVM is to find $\mathbf{W}$ and γ according to the following optimization problem.

$$\max \ \frac{2}{\|\mathbf{W}\|} \ \text{subject to} \ \mathbf{D}(\mathbf{AW}-\mathbf{e}\gamma) \geq \mathbf{e}, \qquad (2.5)$$

where   **D**   is the square diagonal matrix with the diagonal element in the i-th row as the class of the i-th training input;

        A   is the training data matrix whose i-th row corresponds to the i-th training input;

        e   is the column vector where every element in **e** is 1.

The problem of (2.5) is equivalent to

$$\min \ \frac{1}{2}\|\mathbf{W}\|^2 \ \text{subject to} \ \mathbf{D}(\mathbf{AW}-\mathbf{e}\gamma) \geq \mathbf{e}. \qquad (2.6)$$

The optimization problems in (2.5) and (2.6) do not allow any training error, which may lead to overfitting towards the training data. SVM with soft margin is the adaptation of (2.6) to allow some training error and its optimization is as follows.

$$\min \ \frac{1}{2}\|\mathbf{W}\|^2 + \nu \mathbf{e}^{\mathrm{T}}\mathbf{Z} \ \text{subject to} \ \mathbf{D}(\mathbf{AW}-\mathbf{e}\gamma)+\mathbf{Z} \geq \mathbf{e} \ \text{and} \ \mathbf{Z} \geq \mathbf{0} \quad (2.7),$$

where   **Z**   is the column vector containing errors (distance toward the correct bounding plane) of the training data;

        ν is the penalty which determine the severity of error; if ν is high, the penalty of training error will be high.

The optimization of (2.5) - (2.7) can be solved by conventional optimization toolboxes such as CVX [27].

2.1.3.2.2 Ensemble techniques. Ensemble techniques are based on the assumption that multiple classifiers working together yield higher classification accuracy than the single classifier. The ensemble technique improves the classification performance, when the data set is small. It has been used in many biomedical researches and found to be a good classification technique [28-30]. In this study, two ensemble techniques (Bagging and Boosting) were addressed.

Bagging (**B**ootstrap **Agg**regat**ing**), first proposed by Breimen in 1996 [31], is a voting method, where base-learners are made different by the training with slightly different training sets. The generation of base-learners different sets for one training set is done by bootstrap [32]. Subsampling with replacement is applied to the training set in bootstrap. The size of a subsampled set is the same as the one of the training set. Consequently, some training samples may appear more than once and some may not at all. The probability that a sample appears at least once is 0.632. Each base learner is trained with its own subsampled set. Their classification results are combined by a majority vote where the most voted class is the result.

In Boosting, base-learners are created such that they complement one another. The base-learner is trained with the mistakes of the previous learners. There are many variances of Boosting. The original Boosting algorithm was proposed by Schapire in 1990 [33] and is the combination of multiple weak learners. The weak learner has the error probability of less than 0.5, which is better than random guessing in 2-class problem. The combination of weak learners in Boosting leads to much smaller error probability.

AdaBoost (**Ada**ptive **Boost**ing), proposed by Freund and Schapire in 1996 [34], is one of the popular Boosting algorithms. It requires the smaller size of training data than the original Boosting. Initially, every sample in the training data has equal weight. During the training phase, the weights of incorrectly classified samples are increased, while the ones of the correctly classified samples are decreased. The adaptive weight is used to ensure that the error will be corrected. The training is iterative and the updated weight is use for error calculation in the subsequent iteration. In contrast to Bagging where every base-learner is equally important, the base learners in AdaBoost are weighted according to their classification accuracy estimated during the training phase. The classification by AdaBoost for the training data is more accurate than the one by Bagging. If the training set is noisy, AdaBoost will be overfitted to the noise leading to lower accuracy.

2.2 Literature reviews

Academic papers on the treatment of intracranial aneurysm by coil embolization can be classified into three categories: (1) retrospective and prospective studies, (2) in vitro experiments, and (3) the simulation for planning treatment.

2.2.1 Retrospective and prospective studies

The effectiveness of the treatment by coil embolization is often investigated by retrospective studies and prospective studies [35-38]. Volumetric packing rate (VPR) is one of the dominant factors in treatment efficiency. The VPR is defined as the ratio between the coil embolization volume (CEV) and the intracranial aneurysm volume (IAV). Sluzewki *et al.* recommended that the appropriate coil packing rate be about 20-30% in order to reduce an aneurysm recurrence [39], but Piotin *et al.* did not find the relationship between the packing rate and the aneurysm recurrence [40].

The VPR cannot be evaluated in clinical practice because the exact IAV is not known. Therefore, the packing rate is changed to the "radiographic packing rate (RPR)" that is evaluated on two-dimensional fluoroscopic image. Grading scales has been proposed for a broader range of angiographic appearances. There are 6-point grading systems (Figure 2.7). Grade 0 indicates the complete and total aneurysm occlusion without the remnant or interstitial filling within the aneurysm. The higher grade indicates the lower occlusion. The ideal treatment should provide Grade 0 packing density; however, it is difficult to get Grade 0 packing density. In clinical practice, Grade 1 packing density ($\geq$ 90% radiographic density of the aneurysm) is used as the standard for the successful treatment.

2.2.2 In vitro experiments

Before the new endovascular device can be inserted into a human body, the experiment on phantom or in vitro model must be performed. Quantitative knowledge of the relationship between coil packing density and aneurysm inflow can mitigate uncertainties in the evaluation and facilitate the more complete embolization to the aneurysm. When the embolization is incomplete (the blood is not completely occluded), there is a residual flow from the parent vessel into the aneurysm, which may be one factor that contributes to aneurysm recurrence. Numerous studies have investigated the effects of coil embolization on aneurysm fluid dynamics in a silicone

aneurysm model using computational fluid dynamics (CFD) [41-43]. Babiker *et al.* studied the residual flow after a coil placement into a saccular aneurysm at basilar tip under steady flow condition. Their study indicated that the coil embolization was the effective treatment for aneurysms at basilar tip [44]. Goubergrits *et al.* compared the effect of the near-wall flow between an aneurysm with and without coil placement. They founded that even a small VPR embolization significantly altered the near-wall flow in the large part of the aneurysm sac [45].
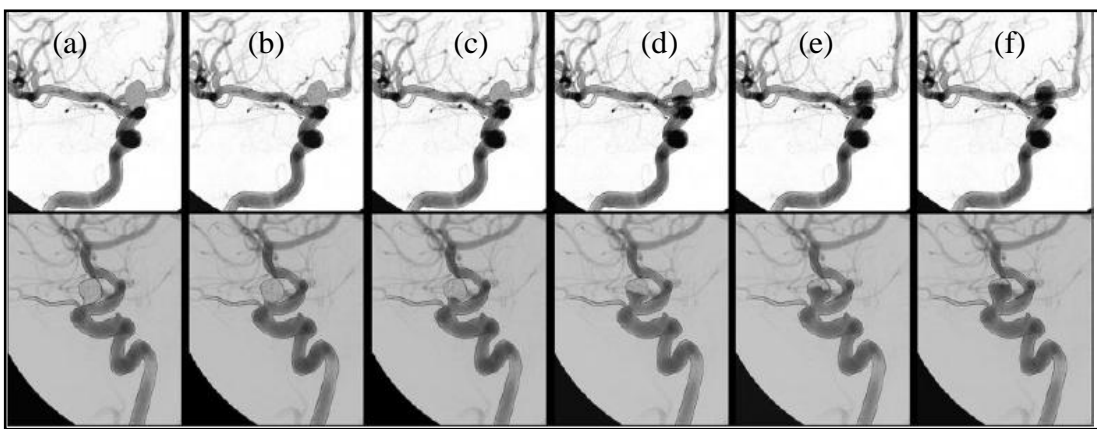
Figure 2.7 Evaluation of radiographic packing rate (RPR) for the occlusion of an endovascular aneurysm on two-dimensional fluoroscopic image; (a) Grade 0: complete aneurysm occlusion, (b) Grade 1: $\geq 90\%$ aneurysm occlusion, (c) Grade 2: 70%-89% aneurysm occlusion, (d) Grade 3: 50%-69% aneurysm occlusion, (e) Grade 4: 25%-49% aneurysm occlusion and (f) Grade 5: $< 25\%$ aneurysm occlusion. [8]

Comparative studies between different types and shapes of an embolized coil are also investigated [4, 46-47]. Piotin *et al.* determined the effectiveness of filling cavity between different material (a platinum coil VS a liquid polymer) [48]. Sugiu *et al.* compared the characteristics of a J-shaped and a helical coils regard to the packing density [49]. They experimented on three irregular aneurysms: dog-ear (Figure 2.8(a)), Mickey Mouse (Figure 2.8(b)) and snowman shapes (Figure 2.8(c)). They suggested that the J-shaped coil was safer and superior in large and irregular aneurysms; whereas, the helical coils were preferable for spherical aneurysms.

Another research topic on in vitro experiment is the optimal volumetric packing density rate (the ratio of coil volume with aneurysm volume). Mandai *et al.* investigated the optimal packing density rate of platinum coils by using the digital

subtraction angiogram (DSA). If the packing ratio is too low, the blood will flow into some part of the sac (Fig. 2.9(a)); whereas, if the packing ratio is too high, the coil will leak into the vessel (Fig. 2.9(b)). They founded that the optimal volumetric packing rate (VPR) was approximately between 26% and 36% [50].
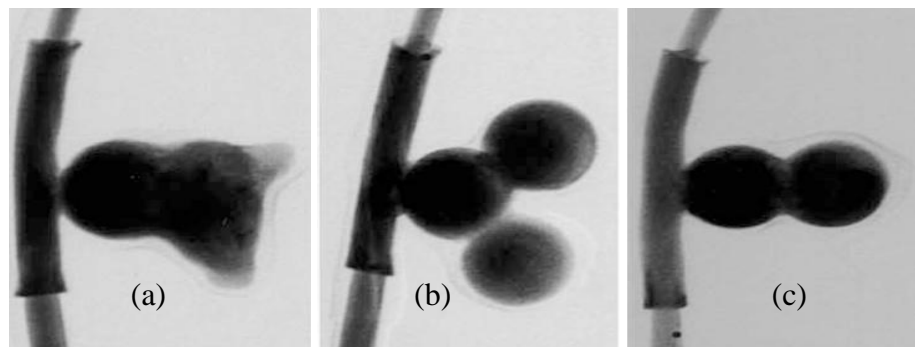
Figure 2.8 Irregular silicone aneurysm in the experiment by Sugiu *et al.*; (a) dog-ear (b) Mickey Mouse and (c) snowman [49].
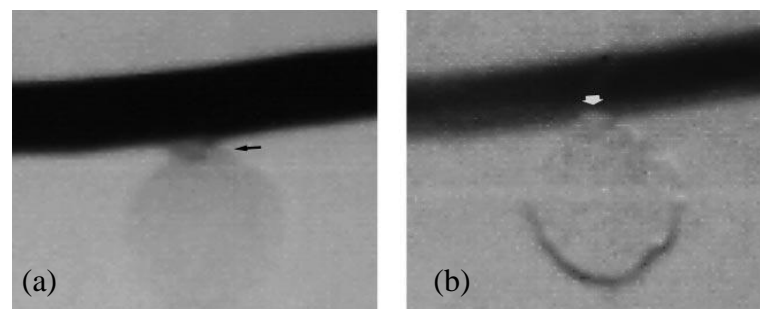
Figure 2.9 The DSA image of (a) minimal dense packing and (b) maximal dense packing. In Figure (a), some diluted contrast medium is seen at (leaked into) the neck, attesting to the suboptimal filling of the sac. In Figure (b), the orifice of the aneurysm is occluded by the coil.

2.2.3 Simulation for planning treatment

Because the success of the treatment by coil embolization depends on the skill of the physician's, some researches offer either a real-time or a near real-time simulation system for training as well as pre-operative planning [51-52]. There is only one study group providing the tool for planning the insertion of the coil [53-54]. The interactive model studies the movement of the first coil deployed into the patient and provides the training tool for physician in controlling the coil. However, most aneurysms required more than one coil placement.

CHAPTER III

METHODOLOGY

The designing process of the proposed methodology is shown in Figure 3.1. There are two main parts: the design of the proposed prediction tools and the in vitro experiment. There are 5 processes in the design of the prediction tools: (1) data collection in Section 3.1.1, (2) feature selection in Section 3.1.2, (3) model construction in Section 3.1.3, (4) model validation in Section 3.1.4 and (5) construction of interactive system in Section 3.1.5. In the in vitro experiment, there are 2 processes: (1) the design of the circulating water system in Section 3.2.1 and (2) construction of a silicone aneurysm in Section 3.2.2.
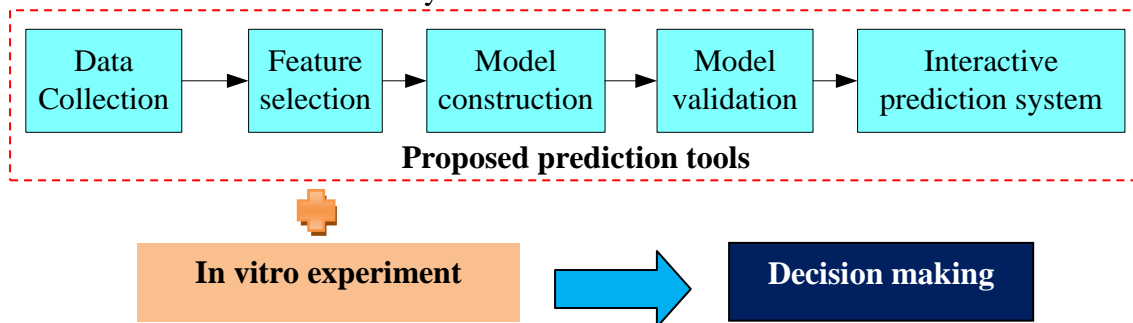
Figure 3.1 Designing process in this study.

3.1 The proposed prediction tools

3.1.1 Data collection

Our Institutional Review Board approved this retrospective study. Patients who had intracranial aneurysms successfully treated by the embolization of platinum bared coils were enrolled in this study. The aneurysm considered had the following characteristics: (1) saccular shape, (2) the length of the dome size of aneurysm (major axis) not exceeding 15 mm and (3) the ratio of the major axis to the minor axis between 0.5 and 2. All data were collected from the division of Interventional Radiology of the King Chulalongkorn Memorial Hospital, Thailand. Database characteristics are shown in Table 3.1. All aneurysms were divided into a training

group ($n_1 = 87$) and a validating group ($n_2 = 13$) using time-interval categorization. Coil placement was performed by one radiologist with general anesthesia at a biplane angiographic system (Ax-Neurostar Plus; Siemens; Germany). Embolized coils in the data sets come from one of the following three manufacturers: Boston Scientific (GDC and Matrix), ev3 (Axium and Nexus), and Codman (Orbit). The training and the validating groups are used to model and validate the prediction tools, respectively.

Table 3.1 Database characteristics in this study

	Training group	Validating group
Collection period	March, 2005 – May, 2011	June, 2011 – January, 2012
Number of patients	82 (62 female, 20 male)	13 (11 female, 2 male)
Number of aneurysms	87	13
Average age ± SD (years)	64.18 ± 13.51	61.23 ± 12.88
Clinical symptom		
Rupture	36 (41.38%)	6 (46.15%)
Unrupture	51 (58.62%)	7 (53.85%)
Aneurysm location		
Basilar tip	23 (26.44%)	5 (38.46%)
PCoA	17 (19.54%)	3 (23.08%)
Cerebral artery	15 (17.24%)	2 (15.38%)
ICA	10 (11.49%)	2 (15.38%)
SCA	8 (9.20%)	-
ACoA	7 (8.05%)	-
Miscellaneous	7 (8.05%)	1 (7.69%)
The number of coil placement		
One coil	14 (16.09%)	1 (7.69%)
Two coils	22 (25.29%)	2 (15.38%)
Three coils	21 (24.14%)	3 (23.08%)
Four coils	13 (14.94%)	4 (30.77%)
Five coils	6 (6.90%)	1 (7.69%)
More than five coils	11 (12.64%)	2 (15.38%)

Note: ACoA = Anterior communicating artery, ICA = internal carotid artery, PCoA = posterior communicating artery, SCA = superior cerebella artery.

In clinical practice, the dominant factor of the coil selection is the shape diameter (SD) of an embolized coil. Physicians first determine the SD and select its length (L) from available coils with the selected SD. In most cases, the longest available L is selected; thus, the selection of L is strongly biased, so in this study, only the SD is investigated.

The training group consisted of 87 aneurysms categorized according to the SD of the coils used in the treatment. The coils were indexed according to the order of insertion. The distribution of the first three embolized coils is shown in Figure 3.2. The figure clearly indicates that the SD usage was not uniform. Some SDs were used more often than the rest.

There are 13 aneurysms in the validating group. The information of the aneurysm's size and the coils used in the treatment is provided in Table 3.2.
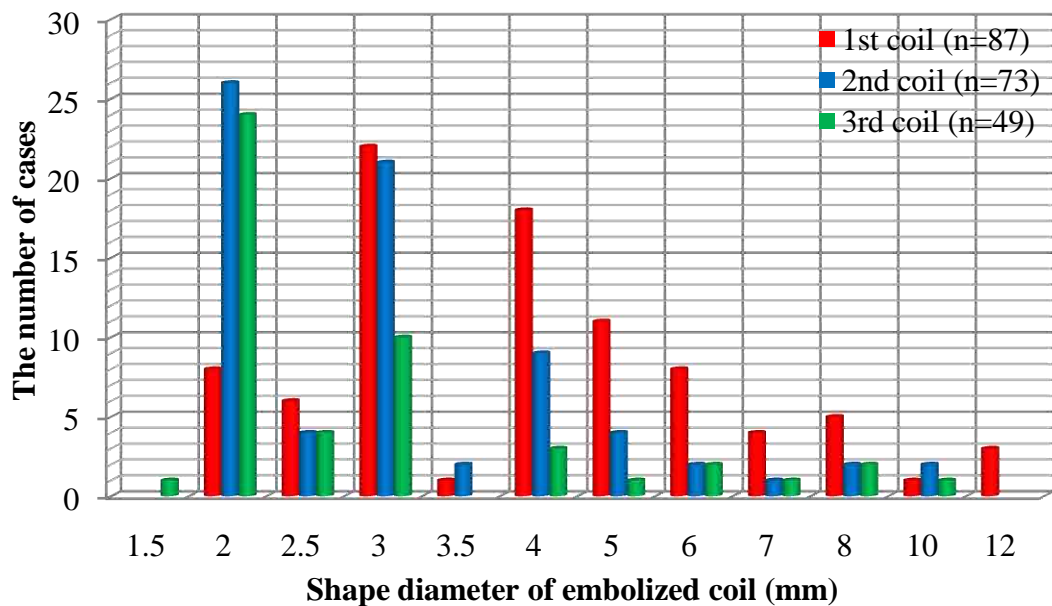
Figure 3.2 The distribution of the training data according to the shape diameter of embolized coils used in the treatment. Coils are indexed according to the order of insertion.

Table 3.2 The size of an aneurysm (in mm) and the size of the first three embolized coils (in mm) in the validating group.

Patient No.	The size of aneurysm (M x N)	The size of an embolized coil (SD x L) (Coils are indexed according to the order of insertion.)		
		1st	2nd	3rd
1	3.8 x 5.6	4x70	3.5 x 75	2.5 x 45
2	3.2 x 2.8	3 x 60	2 x 40	N/A
3	3.0 x 4.0	3 x 100	3 x 60	2 x 30
4	5.8 x 5.1	5 x 200	4 x 120	3 x 80
5	8.3 x 7.3	8 x 300	7 x 300	3 x 200
6	10.0 x 12.0	10 x 300	8 x 300	7 x 200
7	2.2 x 2.6	2 x 80	2 x 40	2 x 40
8	4.5 x 3.9	5 x 100	3 x 60	N/A
9	2.0 x 2.0	3 x 150	N/A	N/A
10	6.5 x 7.4	7 x 300	6 x 200	6 x 200
11	4.0 x 5.0	4 x 70	2 x 20	2 x 15
12	6.0 x 5.0	6 x 200	5 x 150	5 x 150
13	3.0 x 4.0	3 x 80	3 x 60	2 x 60

Note: M = major axis (dome length of aneurysm), N = minor axis (width of aneurysm), SD = shape diameter, L = length, N/A = non-applicable.

3.1.2 Feature selection

Features are the inputs of the prediction system in this study. Their qualities dictate the overall efficiency of the system. The features are chosen according to the selection rules (prior knowledge) of interventional radiologists. The general rules for the coil selection are as follows:

1) The shape diameter (SD) of the first coil is approximately the same as the length of a major axis (the length of aneurysm's dome).

2) The outer diameter (OD) is smaller than the neck of an aneurysm.

3) The length of each coil (L) should be maximized.

4) The treatment has a high chance of success when the radiographic packing rate is more than 90% [8].

5) The volume packing rate (VPR) should be between 26% and 36% [50].

The first rule is the most important rule. It cannot be omitted. The other rules are investigated if they can fit into the system. In the collected database, the length of an aneurysm's neck was rarely measured. The aneurysm was assigned two axes: the major and the minor axes. Figure 3.3 shows three such examples. The major axes of these three aneurysms are 3.0, 6.0 and 13.4 mm, respectively. Without the length of the aneurysm's neck, the second rule cannot be implemented. The second rule is, thus, ignored. The third rule is unrelated to the SD selection; hence, it is not considered. Though radiologists use the fourth rule to check the treatment progress, it is difficult to predict how the embolized coil folds and obstructs the x-ray beam. The fourth rule is, thus, omitted due to the difficulty in estimating the radiographic packing rate. The fifth rule requires the estimation of the volume of the coils and the aneurysm. The volume of the coil can be estimated as

$$\mathrm{CEV} = \frac{\pi(\mathrm{OD})^2 \mathrm{L}}{4}, \tag{3.1}$$

where CEV is the volume of the embolized coil; OD is the outer diameter of $2°$ structure of the embolized coil (Figure 2.4); L is the total length of the embolized coil. The shape of the aneurysm can be approximated as an ellipsoid, so its volume can be calculated as

$$\mathrm{IAV} = \left(\frac{4}{3}\right)\pi\left(\frac{M}{2}\right)\left(\frac{N}{2}\right)\left(\frac{M+N}{4}\right), \tag{3.2}$$

where IAV is the estimated volume of intracranial aneurysm; M and N are the lengths of the major and the minor axes, respectively.
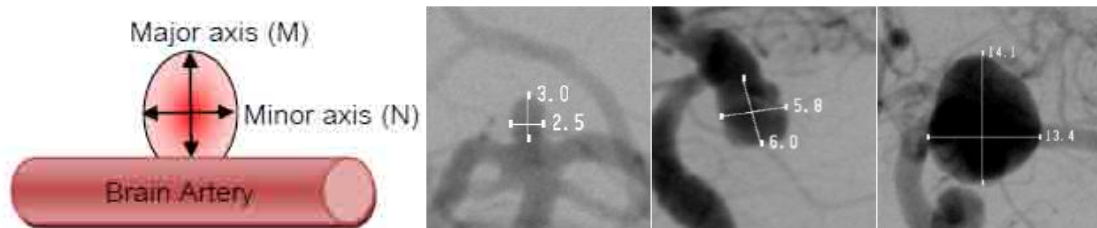
Figure 3.3 Three samples of arteriographic projections used to assess aneurysm dimensions. Major and minor axes were drawn by radiologists.

The selection of the second and the third coils follows similar rules. The major axis becomes the diameter of the space remained after the previous coil has been inserted into an aneurysm. It is necessary to estimate the remaining diameter (RD) and the remaining volume (RV) of an aneurysm. In this study, RD is estimated simply as the difference between the axis and the two times the size of t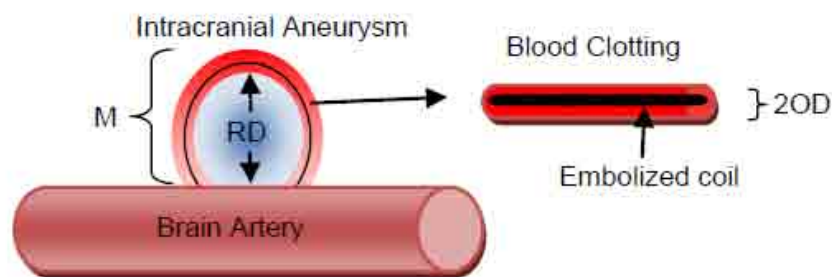he OD (2OD) of the already inserted coils (Figure 3.4). 2OD is the diameter of coil after the blood-clotted enlarging the volume of coil to 400% of its normal size. RV is the difference between IAV and the total CEV of the already inserted coils. The CEV is approximated from the cylindrical volume of the 2° structure (Eq. 3.1).

Figure 3.4 Illustration of the remaining diameter (RD) estimation. The RD is estimated as the difference between the length of the major axis and the diameter of the blood clotted coil (approximated as 2OD).

3.1.3 Model construction

The system is used to model the selection patterns of a radiologist. The following systems are investigated in this study; (1) regression systems, (2) classification systems, and (3) the integrated system of classification and regression (hybrid systems).

3.1.3.1 Regression systems (RS). In regression, all data are combined to create the mapping function between the input and the output. The mapping functions can be of several forms such as linear, polynomial, exponential, etc.

There are 6 RS tested in this study. Since in some cases, only the length of the major axis is used to determine the SD (the first rule in Section 3.1.2). The input of the first three systems in this study is only the length of the major axis. The difference in the three systems is the mapping function. Linear, quadratic and cubic

functions are the mapping function in the first, the second and the third systems, respectively. The fourth system is designed based on the first and the fifth rule in Section 3.1.2; thus, its input is the length of the major axis and the volume of an aneurysm. The volume in Eq. (3.2) is related to the length of the major axis and the one of the minor axis, so in the fifth system, the inputs are the length of the major axis and the one of the minor axis. In the sixth system, it is hypothesized that in addition to the major axis, radiologists also consider the shape of an aneurysm in the SD selection. The shape can be inferred from the ratio between the lengths of the major axis to the one of the minor axis; hence, the inputs of the sixth system are the length of the major axis and the length ratio.

The efficiency of RS depends on the mapping function and the quality of the training data. Generally, the more complex the mapping function is, the better it can represent the training data. This character leads to overfitting if the number of the training data is small. Because there are only 87 aneurysms for the training data, when there are 2 inputs, a linear function with the following form is used as the mapping (predicting) function.

$$SD = a_0 + a_1 x_1 + a_2 x_2 + a_3 x_1 x_2, \tag{3.3}$$

where x_i is the i-th input; SD is the predicted SD; a_0, a_1, a_2 and a_3 are the constants used as the model parameters. The model parameters are often estimated as the value providing the least square error in the training data; therefore, RS has low tolerance to outliers.

3.1.3.2 Classification systems (CS). In classification, all training data are categorized into groups according to the SD. Data in each SD group is used to construct the classification rules for their own group. The classification accuracy depends on the number and the quality of the training data. It is difficult to determine the minimum number of the training data required for the rule construction and to measure the quality of the training data. The general rule is that the higher the number of the training data, the better the classification should be. Another factor affecting the classification accuracy is the classification algorithm. In this study, three supervised

machine learning algorithms were evaluated: Support Vector Machine (SVM), Bagging and Boosting algorithm.

3.1.3.3 Hybrid systems (HS). As shown in Figure 3.2, the distribution of the SD was uneven. Some SDs were rarely used or not used at all; consequently, there were not enough training data to construct the classification rules for the seldom used SDs and the prediction must be done by other methods such as regression. Therefore, coil selection should be considered as the combination of the two problems: (1) the classification problem where the input aneurysm is categorized to the appropriate SD group and (2) the regression problem where the appropriate SD is estimated by the mapping function

In this system, the SDs of embolized coils are separated into two types: the distinct and the ambiguous types. If there are a sufficient number of data in one SD to establish the classification rules, the SD is distinct; otherwise, the SD is ambiguous. The classification rules are established for each distinct SD. The ambiguous SD is assumed to be in one large group and every data with ambiguous SD are used to establish the rule for the ambiguous group. Thus, if there are k distinct SDs, there are classification rules for $k + 1$ groups. SDs in the ambiguous group is predicted by RS.

Figure 3.5 shows the flowchart of the proposed hybrid system. From the input features, the SD is predicted first by CS. If the predicted SD is in the ambiguous group, it is predicted by RS.

The efficiency of HS depends on both RS and CS. Its efficiency will be improved from the system with only the regression or classification, if the benefit of RS and CS are both exploited. In this study, the two systems are integrated after the data is categorized into distinct and ambiguous groups. How the data are categorized becomes the factor affecting the overall efficiency. The optimal configuration is investigated in Chapter 4.
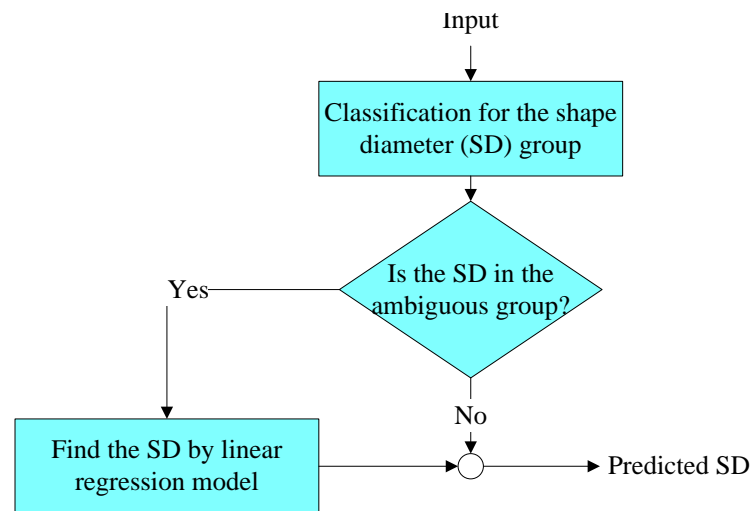
Figure 3.5 The flowchart of the hybrid system for predicting the shape diameter of an embolized coil.

3.1.4 Model validation

The prediction tool is validated based on the predicting accuracy. There are two evaluations: (1) the leave-one-out-cross-validation (LOOCV) and (2) the blind test on the validating set. LOOCV is used to determine the best input features and the function of RS. The blind test is then used to determine the best configuration and to measure the efficiency of HS.

LOOCV is one of the methods to obtain reliable performance estimation when there are not enough data to create additional set for testing [46]. The data set used in this stage was the training data set. For each coil selection, the data of the first (n=87), the second (n=73) and the third coils (n=49) were split into n-1 training and one testing data. RS with the highest predicting accuracy was integrated with different CS in order to construct a hybrid system.

The blind test is used to measure the efficiency of the prediction tool. It is also used to evaluate the hybrid system when different criterion is used to categorize the distinct and the ambiguous SD. In the blind test, the prediction tool was tested with the validating set which contains 13 aneurysms not in the training set. The high accuracy in the blind test indicates that the system provides accurate output from the new (unknown) input (good generality). If the accuracy in the validating set greatly drops in the blind test, it implies overfitting.

3.1.5 Interactive system

Many factors besides the size of an aneurysm affect the SD selection. Examples of the external factor are patients condition, cost, coil availability, etc. Hence, the system giving only one exact SD is not useful, since it does not complied with the actual clinical practice. In this study, the interactive system is proposed as the prediction tool. The possible SDs are suggested. A user then selects SD, which the system uses to estimate the possible SDs of the subsequent coil. The possible SDs are as follows: (1) the output SD from the prediction tool and (2) the SD within 1mm of SD in (1)

The proposed interactive system provides the selected coil in term of the order number. A user is required to choose the product name of an embolized coil. The order number provides the information regarding the SD and the length (L). The order numbers are arranged into 3 categories as follows.

(1) The longest coil with the predicted SD.

(2) Coils with the predicted SD but whose length is not the longest of its SD.

(3) Coil whose SD is within 1mm of the predicted SD and the length is one of the two longest coil of its SD.

Figure 3.6 shows the interface of the proposed interactive system. After a user loads the coil database, the user enters the length of the major and the minor axes of an aneurysm. The volume will be automatically estimated. Then, the user selects the one of the several product names of embolized coil so that the system can provide the set of the possible coils in three categories. After the user selects the coil in the list, the system will provide the set of the possible coils for the next insertion. For example after the user selects the first coil, the system will show the set of the possible second coils (Figure 3.7). Note that the user can select different coil's product name in one aneurysm. Figure 3.8 shows the example of the selection of different coil's product name: the first coil was Axium (QC-10-30-HELIX; 10x300mm; helical shape); the second coil was Orbit (637CF0824; 8x240mm; spherical shape) and the third coil was Matrix (470730-SR; 7x300mm; helical shape).

The packing in the right column of the user interface shows the estimated packing rate for the current selection. However, it is not possible to evaluate the

accuracy without a sufficient number of in vitro experiments. So this part will not be evaluated.
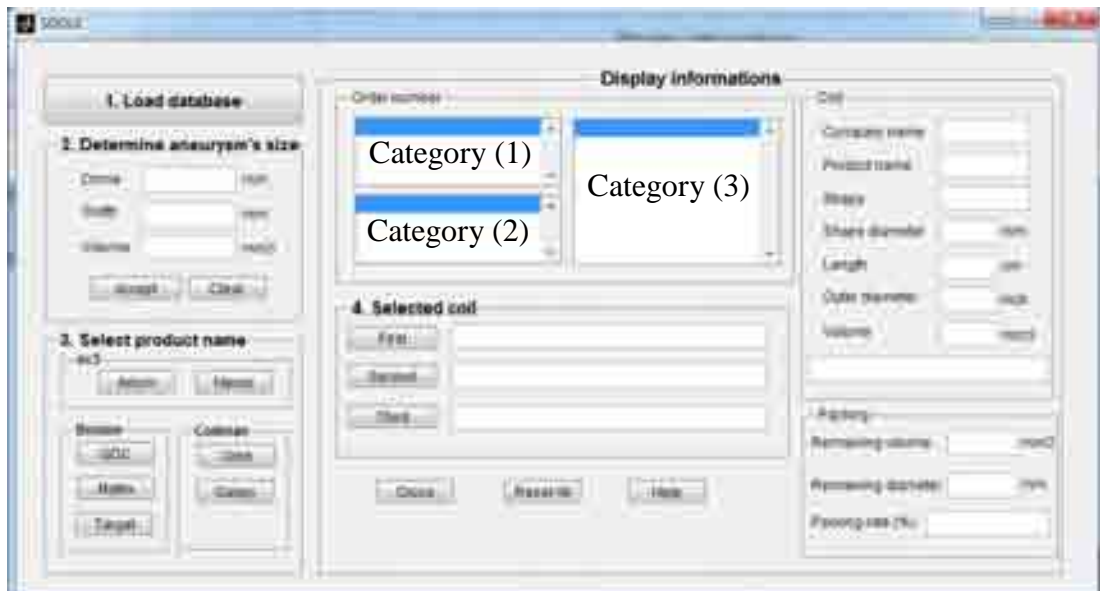
Figure 3.6 The interface of the proposed interactive system.
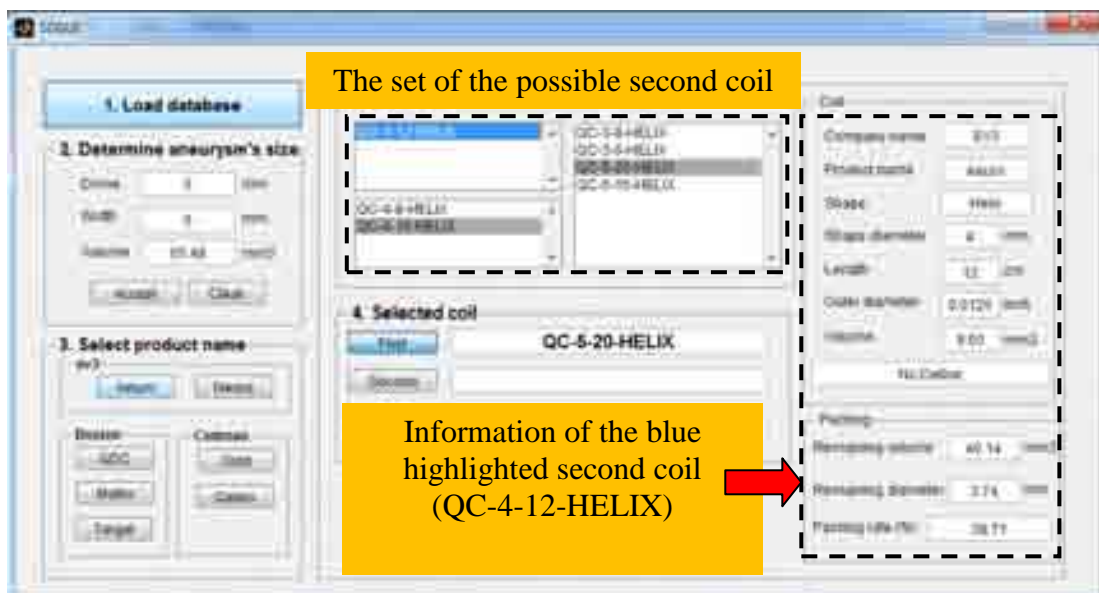
Figure 3.7 A set of the possible second coil after the first coil has been selected. The information of the selected coil (blue tab) is automatically displayed.

Figure 3.8 Example of the selection with different coil's product name in one aneurysm.

3.2 In vitro experiment

Though the blind test evaluation of the interactive system provides some confidence for the accuracy of the coil selection, in vitro experiment is also performed to further guarantee the efficiency. Due to the very high cost of embolized coils (more than 20,000 Thai baht per coil), the number of the experiment is limited to three.
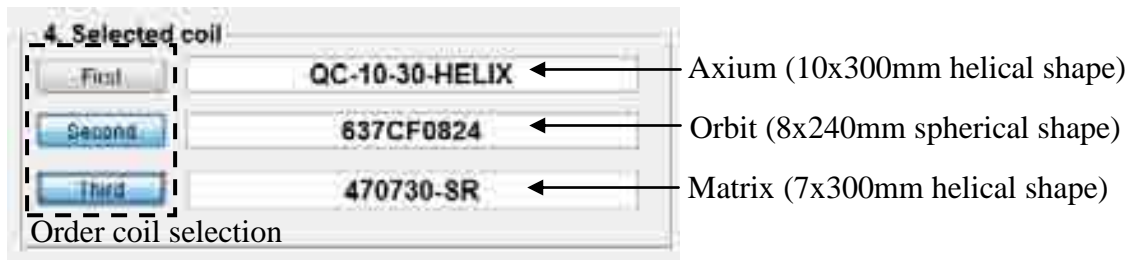
3.2.1 Design of the circulating water system

Figure 3.9 shows the circulating water system for in vitro experiment. The circulating water system consists of silicone tube and water pump. The silicone tube with an internal lumen of 5mm is used as the artificial blood vessel. The silicone aneurysm is attached to the tubes by silicone. A stationary flow is obtained by using a sealless magnetic pump (Sanso; PMD-211). The stationary flow can be used because the objective of this experiment is not to evaluate the fluid mechanism inside the aneurysm but to measure the properness of the size of the coil. The flow is necessary only to avoid the coil from sticking to the vessel. A valve is used to control the flow rate to approximately 750 ml/min to match the actual physiological conditions [57]. As in the actual clinical operation, the experiment is performed under the guideline of a biplane angiographic system (Ax-Neurostar Plus; Siemens; Germany). The system is located at the division of Interventional Radiology, King Chulalongkorn Memorial Hospital, Thailand.

Figure 3.10 shows the experimental setup. The combination of the guidewire (SilverSpeed®-10; ev3) with microcatheter (Echelon™-10; ev3) is retained within the circulating water system and is placed into the silicone aneurysm so that its tip was just at the level of the orifice of the aneurysm. Then the stepwise filling of the sac is performed by filling contrast medium under a biplane angiographic system until the

surface of the fluid is just at the orifice level. This infusion is used for measuring the two axes in a single two-dimensional image.
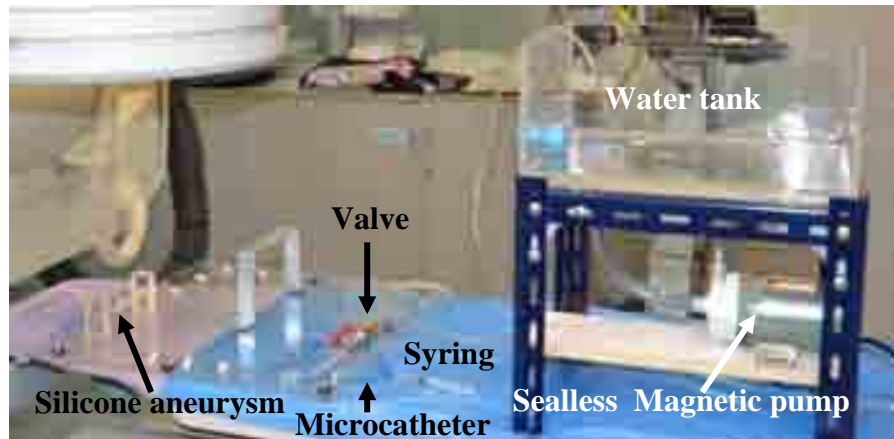
Figure 3.9 Circulating water system

Figure 3.10 in vitro experiments under biplane fluoroscopic system at the division of Interventional Radiology, King Chulalongkorn Memorial Hospital, Thailand.

3.2.2 Building of silicone aneurysm

Two different kinds of in vitro silicone side-wall aneurysm models were made by painting silicone on an aneurysm mold. The structure of a prototype mold was created by using SolidWorks V.2011 (Solid Works Corp.). The structure was then imported into the 3D printer (Z-printer® 450 model, Figure 3.11) to create the prototype mold. The structures of the prototype molds used in this experiment are

shown in Figure 3.12. The unit is in mm. The aneurysm molds had a lateral spherical aneurysm cavity with the internal diameter of 5mm for the small type (neck = 2mm) and 10mm for the medium type (neck = 4mm). Figure 3.13 shows the silicone aneurysms after they were attached to the tubes. In order to match the actual clinic operation, the size of two silicone aneurysms were determined by measuring diameter of two axes (major and minor axes) on biplane angiographic system as shown in Figure 3.14(a) and 3.14(b), respectively.

Figure 3.11 Zprinter® 450 models for constructing aneurysm mold

Photograph	Side view	Top view
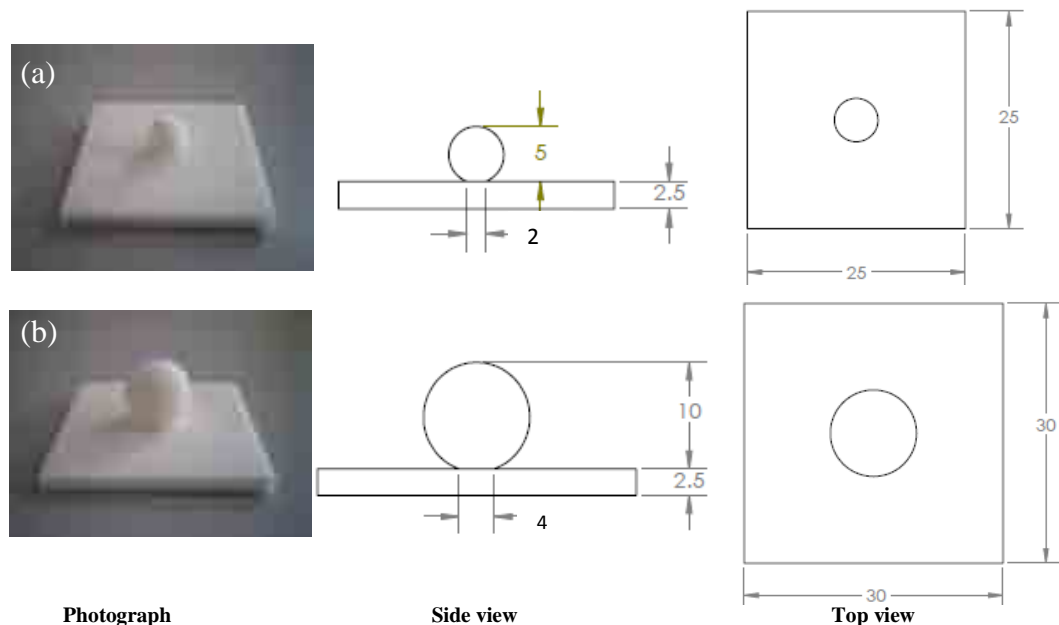
Figure 3.12 Photograph and structural detail of aneurysm mold in top view and side view (a) 5mm (b) 10mm
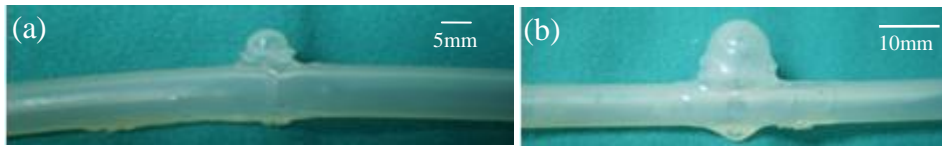
Figure 3.13 Soft silicone models of sidewall aneurysms: (a) 5mm diameter model (b) 10mm diameter model.
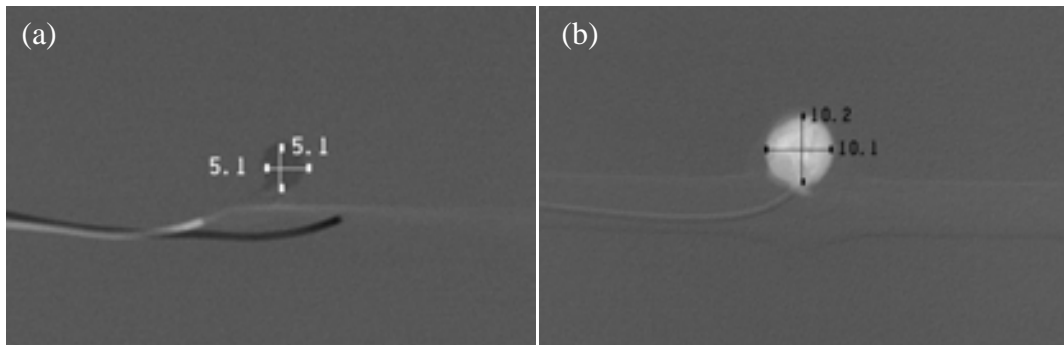
Figure 3.14 The measurement of the two axes of the silicone aneurysm in biplane angiographic imaging: (a) 5mm diameter and (b) 10mm diameter models.

CHAPTER IV

RESULTS

4.1 Model validation

The leave-one-out cross validation (LOOCV) was used to measure the efficiency of each model. In this method, n-1 data from the training dataset were used to construct the model; the remaining one datum was used to validate the efficiency of the model. It was performed n times using a different datum for validation. In this study, the predicting accuracy was used as an evaluation matrix. Coils were indexed according to the order of insertion.

4.1.1 Regression system (RS)

Figure 4.1 shows the performance comparison of six regression models. The performance of models using only the major axis (M) as the only input (the first, the second and the third systems) were poor with the accuracy less than 30% in all cases. It was also revealed that complex functions had the lower performance than the simple linear function. The other three models using the input pair had approximately the same accuracy. The maximum accuracy among the system with two inputs was the model using M and the volume (V) as the inputs. However, the difference was not significant.

RS provided the fairly high accuracy for the first coil prediction (68%); however, its accuracy sharply dropped in the second and the third coils prediction (less than 30% in both cases).

The result of LOOCV indicates that though RS was a fairly good model for the first coil prediction, it was not so for the second and the third coil prediction. Furthermore, the information of M is not sufficient. The shape of an aneurysm in term of the minor axis should be included.
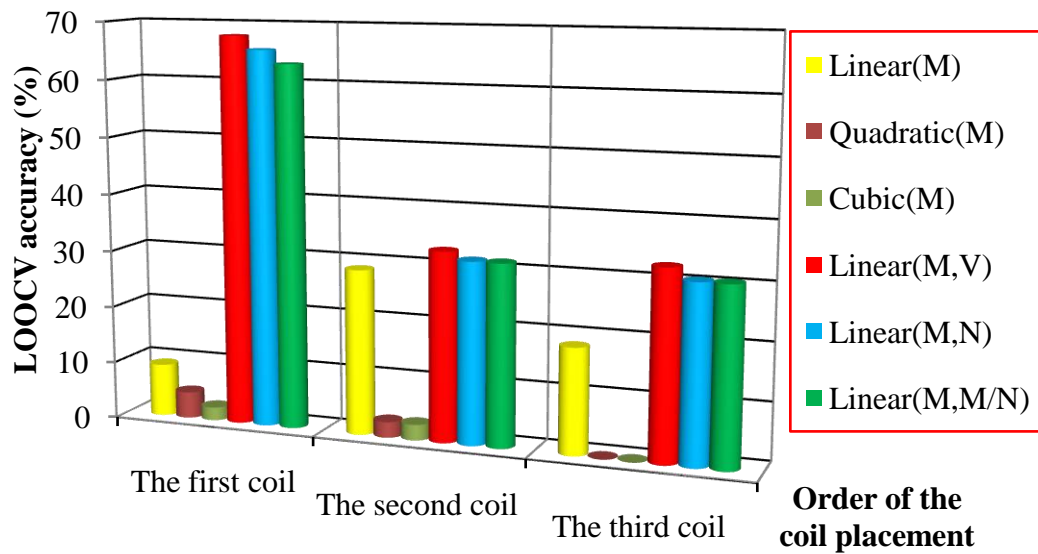
Figure 4.1 The predicting accuracy of the first three coils by different regression functions. Leave-one-out cross-validation method was used for the evaluation. The input of the function is shown inside the parenthesis where M, N and V represent major axis, minor axis and volume, respectively.

4.1.2 Classification system (CS)

In this study, CSs by the following three supervised machine learning techniques were compared: Bagging, Boosting and SVM techniques. Figure 4.2 shows the performance comparison of these three CSs. In the first coil prediction, the classification by Bagging technique provided the highest accuracy (59%), which was much higher than the other two techniques. There was no district difference among the three systems in the prediction of the second coil prediction. The accuracy was approximately 40%. In the third coil prediction, the classification by SVM technique provided the highest predicting accuracy (49%), while the classification by Bagging technique provided the lowest accuracy (39%).

The results of LOOCV indicate that in the second and the third coil prediction, CS provided approximately 10% higher predicting accuracy than RS. However, the accuracy was less than 50%. As for the first coil prediction, RS provided better prediction than CS. The low predicting accuracy of the first coil was the result of that CS requires the sufficient number of training data to establish classification rule;

however, the SD distribution was uneven and some SDs did not have enough training data to establish the rules.

Figure 4.2 The predicting accuracy of the first three coils by different classification techniques. Leave-one-out cross-validation method was used for the evaluation.

4.1.3 Hybrid system (HS)

HS combines RS and CS in order to exploit the advantage of both techniques. The model in RS was the linear function with the inputs of M and V. As for CS, Bagging, Boosting and SVM techniques were all investigated, because there was no clear winner in the experiment in Section 4.1.2. Figure 4.3 shows the performance comparison of HS. The highest accuracy was achieved in the model using Bagging technique for classification. The accuracies were 77%, 77%, 65% for the first, the second and the third coil prediction, respectively. The accuracies in all cases were much higher than the other two models which had the predicting accuracy of 40-50% in all cases.

The result showed the improvement in predicting accuracy over RS and CS. Furthermore, the performance drop in the second and the third coil prediction was less. One of the causes of the performance drop was the error in approximating remaining diameter (RD) and remaining volume (RV). It was impossible to measure the correct the RD and RV in vivo; thus, the error cannot be avoided. The lower performance drop indicated that HS had higher tolerance against such error.
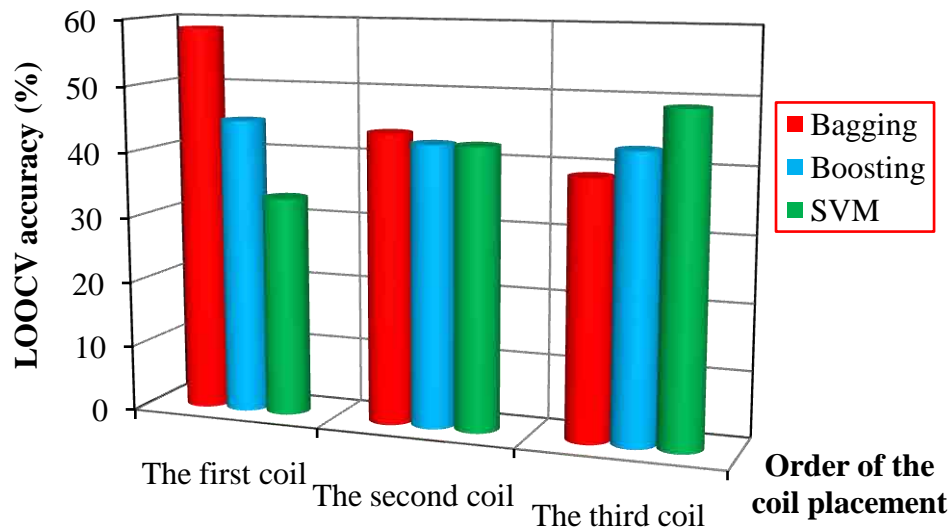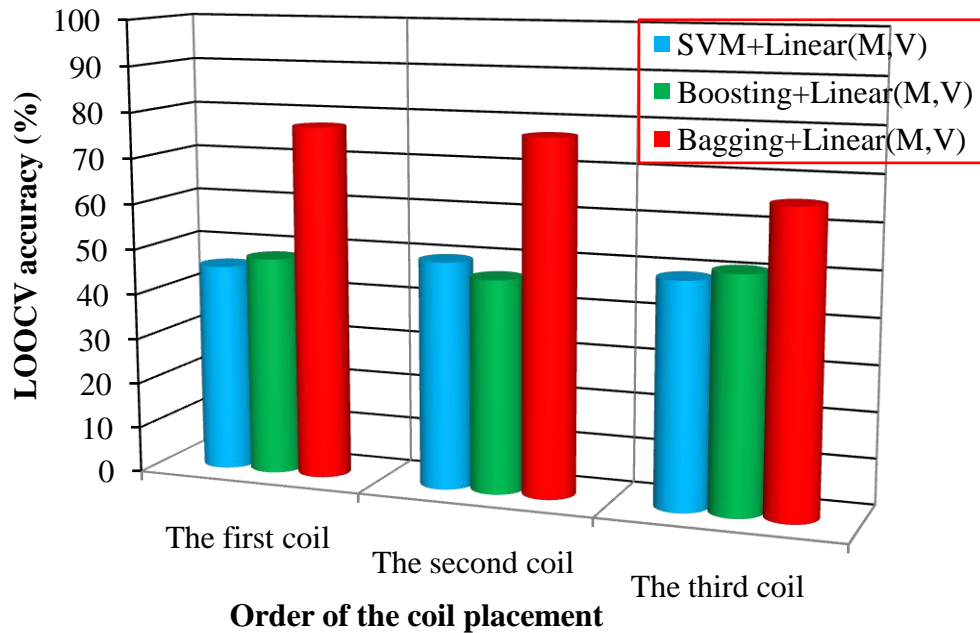
Figure 4.3 The predicting accuracy of the first three coils by different hybrid systems. Leave-one-out cross-validation method was used for the evaluation.

4.2 Parameter evaluation

HS uses CS to classify an input aneurysm to either a distinct SD group or an ambiguous group. RS is then used to predict the SD of the coil classified to the ambiguous group. The number of available training data is used as the criterion to categorize the SD into the distinct and the ambiguous groups. In the training dataset, if the number of treatments using the SD is more than the predefined threshold, the SD will be considered distinct; otherwise, it belongs to ambiguous group.

The evaluation for the optimal threshold was performed on the validating set. Table 4.1 shows the predicting accuracy at different thresholds. The threshold was determined according to the number of available data. In the prediction of the first coil, RS and HS with the threshold of 22 gave the highest accuracy. In the prediction of the second coil, as in LOOCV, the performance of RS was highly degraded. The highest accuracy was achieved by HS when the threshold was set larger than 9. In the prediction of the third coil, the highest accuracy was achieved when the threshold was less than 24.

Since the speed of RS is faster than CS and HS, it should be implemented whenever the accuracy is approximately the same as CS and HS. So RS should be implemented as the first coil prediction.

There are a number of possible hybrid systems (with different threshold) for the second and the third coil prediction. In addition to the accuracy, the error in SD size should be considered. In the second coil prediction, the threshold of 26 provided the best result. In the third coil prediction, the threshold of 10 provided the best result.

The threshold was investigated further by evaluating the effect of adding a distinct group into CS. In the second coil prediction, when the threshold was decreased to 9, the SD prediction of the 7th patient (actual SD = 7mm) changed from 6.17mm to 4mm. 4mm SD was the distinct group added to the system at the threshold of less than or equal to 9. Thus, the addition of the group at the threshold $\leq$ 9 led to larger error. Therefore, in the second coil prediction, the threshold should be kept larger than 9.

In the third coil prediction, when the threshold was decreased from 10 to 4, 2.5mm SD was added as the distinct SD. However, the addition of 2.5mm SD did not provide the improvement for the prediction of the 1st patient (actual SD = 2.5mm). Thus, it was unnecessary to create the additional group. The threshold should then kept at 10 where the addition of 3mm SD group led to better prediction as shown in the 3rd patient.

The SD difference of 1mm is acceptable in this study. With this relaxation, every prediction of the first and the second (threshold = 21) coils was acceptable. In the prediction of the third coil (threshold = 10), the predictions of the 10th and the 12th patient were unacceptable. In both treatments, there were two coils of the same SD. The cause of the error is in the design of RD for the second and the third coil predictions. RD will be reduced, whenever the new coil is inserted. The system is, therefore, biased such that the subsequent coil should have smaller SD than coils already inserted into an aneurysm.

Table 4.1 The results of SD prediction (in mm) using different threshold value. The output SD is predicted by combination between classification and regression (yellow label). (N/A is non-applicable)

SD of the first coil (mm) — Predicted under Threshold values: 3, 4, 5, 6, 8, 11, 18, 22

Patient no.	Actual	Predicted (classification)	Output (regression, yellow)	RS
1	4	4	3.72	3.84
2	3	3		3.15
3	3	3		3.03
4	5	4	4.87	5.03
5	8	8	7.90	8.05
6	10		10.39	10.34
7	2	2	2.28	2.30
8	5	5	4.25	4.33
9	3	2	2.11	2.12
10	7	6	6.27	6.49
11	4	4	3.87	3.97
12	6	6	5.60	5.73
13	3	3		3.03

SD of the second coil (mm) — Predicted under Threshold values: 2, 4, 9, 21, 26

Patient no.	Actual	Predicted (classification)	Output (regression, yellow)	RS
1	3.5	3	3.05	2.90
2	2	2		2.26
3	3	2		2.33
4	4	3	3.80	3.32
5	7	4	6.17	5.24
6	8		8.91	8.89
7	2	2		1.99
8	3	3	3.30	2.76
9	N/A	N/A	N/A	N/A
10	6	5	4.89	4.40
11	2	3	3.11	2.85
12	5	4	4.29	3.48
13	3	2		2.34

SD of the third coil (mm) — Predicted under Threshold values: 2, 3, 4, 10, 24

Patient no.	Actual	Predicted (classification)	Output (regression, yellow)	RS
1	2.5	3	1.80	2.45
2	N/A	N/A	N/A	N/A
3	2	2		1.83
4	3	3	2.64	2.62
5	3	3	4.69	4.42
6	7	8	7.77	8.36
7	2	2		1.53
8	N/A	N/A	N/A	N/A
9	N/A	N/A	N/A	N/A
10	6	4	3.42	3.58
11	2	2		2.35
12	5	3	2.81	2.71
13	2	2		1.86

4.3 Evaluation of the interactive system

The interactive system described in Section 3.1.5 was implemented with RS as the first coil prediction and HS as the second and the third coil prediction. The threshold of HS in the second and the third coil prediction were both set at 10.

Figure 4.4 shows the predicting accuracy of the interactive system. In the first coil prediction, even though the radiologist did not always use the coil with the predicted SD (the first and the second choices), his choice of SD was within the acceptable bound of 1mm. Thus, the predicting accuracy was 100% when all three choices were considered.
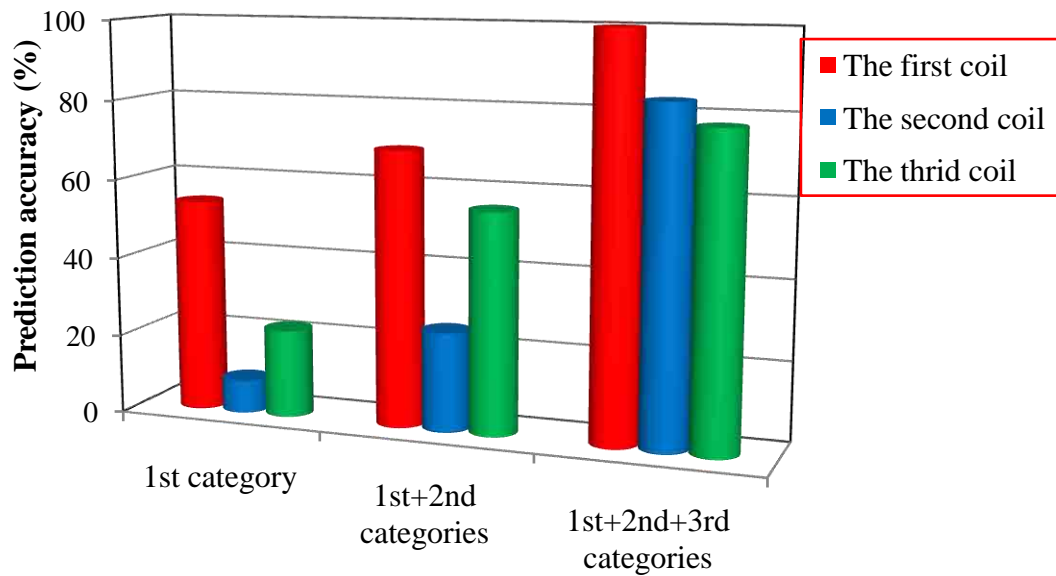
In the second coil prediction, the predicting accuracy was 83% when all three choices were considered. Further investigation revealed that the error was caused by the incorrect L selection. L used in the actual treatment was not within the two longest available L.

In the third coil prediction, the predicting accuracy was 78% when all three choices were considered. Because the SD variation of the third coil was small, the radiologist had the higher tend to select the predicted SD in the third coil than in the second coil. The error in the third coil selection was caused by the incorrect SD selection. Furthermore, there was one case that the system could not be used due to the selection failure of the second coil.

In addition to the coil selection, the estimated packing rate (shown in the bottom right of the Figure 3.6) was also investigated. However, there was no correlation that could be established.

4.4 In vitro experiment

The prediction of the interactive system was evaluated on two artificial aneurysms: (1) small spherical aneurysm with the major and the minor axes of 5.1mm (Figure 3.14(a)) and (2) medium spherical aneurysm with the major axis of 10.2mm and the minor axis of 10.1mm (Figure 3.14(b)). The two aneurysms were packed with coils in the first category (the predicted SD with the longest L). Figures 4.5 and 4.6 show the biplane angiography image after each coil was placed inside the small and the medium aneurysm, respectively. In the small aneurysm, only two coils could be packed inside. The estimated volumetric packing rate (VPR) was 36.48%.

Figure 4.4 The predicting accuracy of the interactive system

The slight coil protrusion would not lead to the health problem because it could be cut in the real operation. The coil embolization in the medium aneurysm was packed without the risk of coil protrusion. It should be noted that in the actual operation, additional coils should be embolized into the medium aneurysm.

One precaution regarding the treatment of an aneurysm with coil embolization is to avoid using coil that is too large as it can cause the protrusion of embolized coils. In this experiment, the small aneurysm was packed such that the first two coils were the largest coil recommended by the interactive system, i.e. the coil whose SD was 1mm larger than the predicted SD and the length was the longest for its SD. Figure 4.7 shows the biplane angiography image after each coil placement. All coils could be packed inside without causing the rupture. Table 4.2 shows the list of the coil embolized into the aneurysm models.
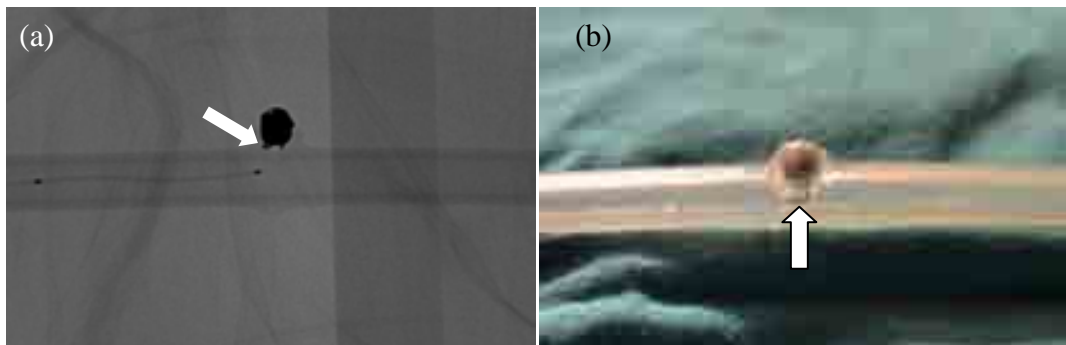
Figure 4.5 Biplane angiography image of the small silicone aneurysm (M = N = 5.1mm) in the second experiment after (a) the first and the second coil placement (5x200mm and 4x120mm, respectively). (b) The photograph after the placement of the two coils. Arrow in (a) and (b) show the slight coil protrusion found after the insertion of the second coil.
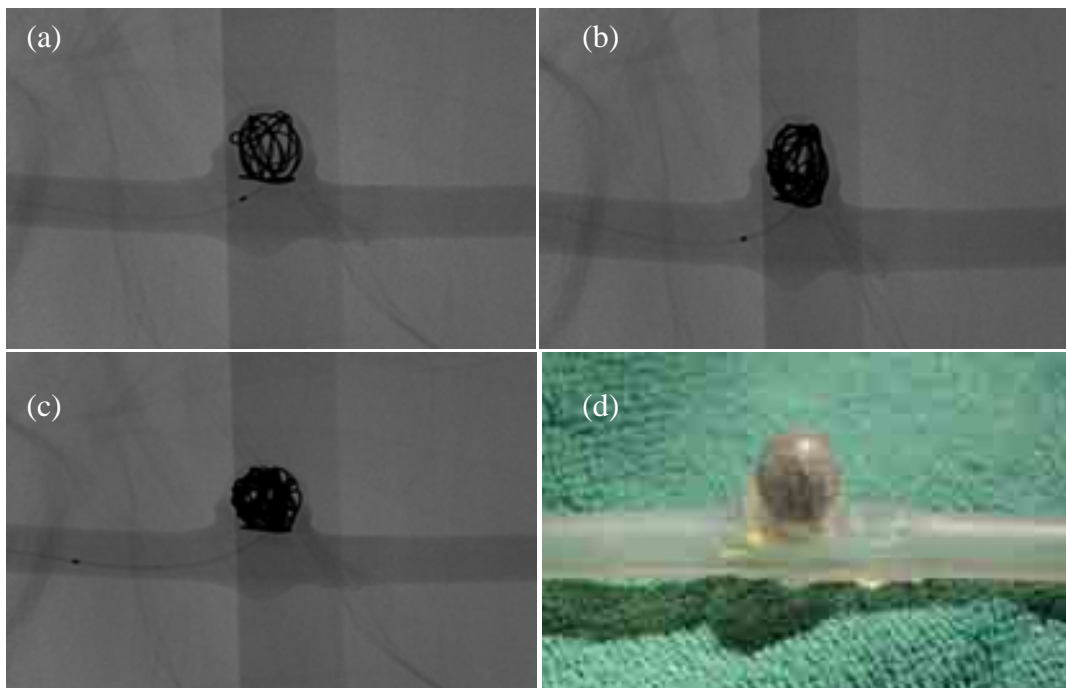
Figure 4.5 Biplane angiography image of the medium silicone aneurysm (M = 10.2mm, N = 10.1mm) after (a) the first coil placement (10x300mm), (b) the second coil placement (8x300mm) and (c) the third coil placement (7x300mm). (d) The photograph after the placement of the three coils.
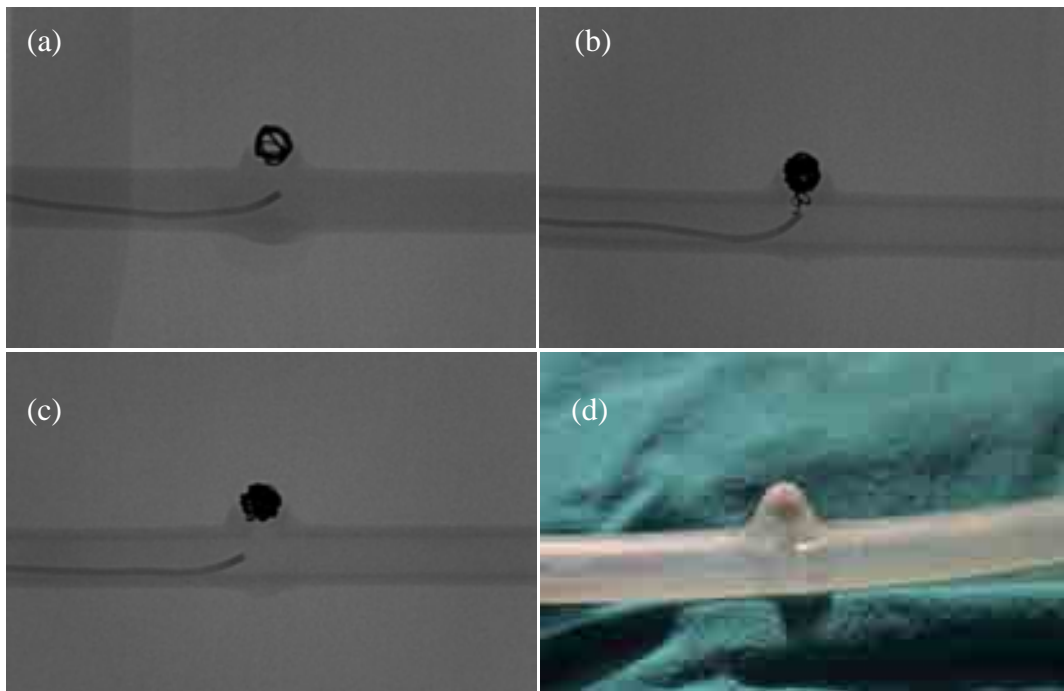
Figure 4.7 Biplane angiography image of the small silicone aneurysm (M = N = 5.1mm) after (a) the first coil placement (6x120mm), (b) the second coil placement (5x100mm) and (c) the third coil placement (3x30mm). (d) The photograph after the placement of the three coils.

Table 4.2 List of the coil embolized into the silicone aneurysm in the in vitro study.

Order of insertion	Order number of coil {SD(mm) x L(mm)}	Category index	Estimated VPR (%)
Experiment 1. Small silicone aneurysm (M = N = 5.1mm)			
The first coil	QC-5-20-HELIX {5x200}	1	22.80
The second coil	QC-4-12-HELIX {4x120}	1	36.48
Experiment 2. Medium silicone aneurysm (M = 10.2mm, N = 10.1mm)			
The first coil	QC-10-30-HELIX {10x300}	1	5.06
The second coil	QC-8-30-HELIX {8x300}	1	10.12
The third coil	QC-7-30-HELIX {7x300}	1	15.18
Experiment 3. Small silicone aneurysm (M = N = 5.1mm)			
The first coil	X-6-12-T10-TC {6x120}	3	8.75
The second coil	X-5-10-T10-TC {5x100}	3	16.05
The third coil	X-3-3-T10-HSS {3x30}	2	18.24

CHAPTER V

DISCUSSION, CONCLUSION AND RECOMMADATION

5.1 Discussion

5.1.1 Model evaluation

The regression system (RS) was the simple prediction system, yet it was proved to be a good prediction of the first coil. However, its performance dropped to become the worst predictions of the second and the third coils. The classification system (CS) had lower performance drop from the first to the second coil prediction; however, its performance was not impressive with the predicting accuracy of less than 50% in most cases. The cause of the performance drop in the second and the third coil placement was the inaccurate estimation of the remaining diameter (RD) and the remaining value (RV). The error is considered as noise in machine learning system; thus, the results indicate that CS had higher tolerance to noise than RS. By incorporating CS into RS, the hybrid system (HS) provides the highest predicting accuracy for the second and the third coil prediction.

SVM has been successfully implemented as classification techniques in many biomedical researches [58-61]; however, the integration of SVM in HS did not provide a good result. This could be because the number of the training data was small, as SVM is not well equipped with the algorithm to establish the classification rules with the small number of training data. The ensemble methods (Bagging and Boosting) are designed to solve the small-training-data problem and are recommended for classification technique.

The integration of classification by Bagging technique to RS provided the highest predicting accuracy in all cases in the prediction of the second and the third coil. Bagging was suggested for implementation with a high level of noise distribution in training data [62-63]. The much lower performance of HS with Boosting technique indicated that the data were noisy. In addition to the inaccurate RD and RV, the noise

also came from the incomplete inputs which are the factors that the radiologist considers besides the size of the aneurysm. The high performance difference between Bagging and Boosting implied that this factor should not be omitted.

5.1.2 Parameter evaluation

The performance of HS regarding the predicting accuracy was quite stable with the change of the threshold (to categorize the shape diameter (SD) to the distinct and the ambiguous group). This is a desirable property of the system. The experiment on the validation dataset indicates that the threshold for the second and the third coil prediction should be set at least 10. However, the exact value could not be given, due to the small number of the validating dataset. As for the first coil selection, the use of raw data reduced the need for the noise tolerance of CS, so RS could be applied.

There were 2 cases that the system failed to predict the SD within the 1mm error bound. Both of them were the cases that more than one coil of the same SD were used in the single patient. The cause of the failure was the strong bias to reduce the coils size in RD.

5.1.3 Evaluation of the interactive system

There were two causes of prediction failure in the interactive system. The first one was the SD prediction error as mentioned in Section 5.1.2. The second one is the use of the simple rule for the length (L) selection. It is difficult to train for the function of L, because in most cases in the dataset, the longest available L was used. Though the volume can be used to limit L, no correlation between the packing rate and the number of the coils used in the treatment was found in the experiment. The lack of correlation indicates that some modification to the approximated volumes in Eqs. 3.1 and 3.2 is necessary before the volume could be used to estimate L.

5.1.4 In vitro experiment

The predicted SD from the interactive system was validated by the in vitro experiment. In the first two experiments, the small and the medium spherical aneurysms were packed with the coils recommended as the first category of the interactive system. In the third experiment, the small spherical aneurysm was packed such that the first two coils were the largest recommended coils. Coils were

effectively packed inside the aneurysms without the risk of coil protrusion in two cases. The experiment demonstrated the safety and the effectiveness of the interactive system in predicting the size of the first three coils.

There was some coil protrusion in the first experiment on the small spherical aneurysm. The protrusion indicated that the shorter coil should be used. According to the research of Piotin *et al* [50], the maximum packing rate was 36.15%. In this experiment, the approximated packing ratio was 36.48%. The volumetric packing rate (VPR) should be integrated into the rule for L selection.

5.2 Conclusion

This study proposed the system for selecting SD of the first three embolized coils in the treatment of an intracranial aneurysm. RS based on the pairwise interaction between the major axis and the volume was use as the guidance for the selection of the first coil. HS using Bagging classification and RS (pairwise interactive between major axis and aneurysm' volume) was used for the selection of the second and the third coil. Bagging classification was used to select SD which had at least 10 training data. The inputs of the system were the length of the major and the minor axes. The experiment showed that the system could be used to provide the predicted SD within 1mm of the actually used SD with the probability of 1, 1 and 0.8 for the first, the second and the third coil, respectively.

The interactive system for SD selection was implemented. In this system, the user can select SD that is within 1mm of the predicted SD as radiologists may select the smaller or larger SD to accommodate the external factors. The in vitro experiment was then performed to demonstrate that there was no risk of coil protrusion when the largest coil provided by the interactive system was used.

5.3 Recommendation

- Though the number of training data was moderated, most publishing papers exhibited a large number of training data for model improvement. Moreover, the size of the blind test was only thirteen. The recommendation for the size of the distinct SD could not be strongly established.

- For the first coil prediction, both RS and HS can be used. However, RS is recommended because it is faster.

- For the second and the third coil prediction, HS should be applied. Bagging should be used as the classification technique.

5.4 Future works

The experiment indicates that the system was biased such that the SD of the subsequent coil must be smaller. Since in some treatments, there were more than one coils of the same SD, the system failed to provide the correct prediction. The modification of RD function to reduce the bias should be investigated.

In the interactive system, it is necessary to add the function that allows users to insert their selected SD and L, in case that their selection is not available in the output box; otherwise, the system cannot be used for the prediction of the subsequent coil

REFERENCES

[1] Bederson, J.B.; Connolly, E.S.; Batjer, H.H.; et al. (2009). Guidelines for the management of aneurysm subarachnoid hemorrhage: A Statement for Healthcare Professionals from a Special Writing Group of the Stroke Council, American Heart Association. Stoke 40: 994-1025.

[2] Guglielmi G. (2009). History of the genesis of detachable coils: A review. J Neurosurg 111: 1-8.

[3] Johnston, S.C.; Higashida, R.T.; Barrow, D.L.; et al. (2002). Recommendations for the endovascular treatment of intracranial aneurysms: a statement for healthcare professionals from the Committee on Cerebrovascular Imaging of the American Heart Association Council on Cardiovascular Radiology. Stoke 33: 2536-2544.

[4] Matsubara, N.; Miyachi, S.; Nagano, Y.; et al. (2011). Evaluation of the characteristics of various types of coils for the embolization of intracranial aneurysms with an optical pressure sensor system. Neuroradiology 53: 169-175.

[5] Sang, Y.K.; Sung, K.M.; Dae, C.J.; et. al. (2011). Pre-operative of advanced prostatic cancer using clinical decision support systems: Accuracy comparison between support vector machine and artificial neural network. Korean J Radiol. 12(5): 588-594.

[6] Mosby's Medical Dictionary. Cerebral aneurysm [Online]. 2009. Available from: http://www.medicaldictionary.thefreedictionary.com/cerebral-aneurysm.html [2012, April 24]

[7] SNIS. Aneurysm: What is an aneurysm? [Online]. 2010. Available from: http://www.snisonline.org. [2012, April 10]

[8] Meyers, P.M.; Schumacher, H.C.; Higashida, R.T.; et al. (2010). Reporting standards for endovascular repair of saccular intracranial cerebral aneurysms. Am J Neuro Radiol 31: E12-E24.

[9] Mountain View Hospital. Health information: aneurysm [Online]. 2012. Available from: http://www.elcaminohospital.org/Heart_Vascular_Institute/Cardiovascular_Health_Information/Aneurysm.html. [2012, April 24]

[10] Vega, C.; Kwoon, J.V.; and Lavine, S.D. (2002). Intracranial aneurysms: current evidence and clinical practice. Am Fam Physician 66(4): 601-609.

[11] Im, S.H.; Han, M.H.; Kwon, O.K.; et. al. (2009). Endovascular coil embolization of 435 small asymptomatic unruptured intracranial aneurysms: procedural morbidity and patient outcome. Am J Neuroradiol. 30: 79-84.

[12] Kil, S.C.; Pyoung, J.; Keon, H.K.; Sung, T.K.; Hyung, J.K.; and Hong, S.B. (2010). Endovascular coil embolization of vary small intracranial aneurysm. Korean J Radiol 11: 536-541.

[13] Rooij, W.J.V.; Sluzewki, M. (2006). Packing density in coiling of small intracranial aneurysms. Am J Neuro Radio 27: 725-726.

[14] Yu, S.C.H.; Wong, W.C.K.; Chung, A.C.S. (2007). A Losse-packing approach for coil embolization of giant intracranial aneurysm. Asian J Surg 30(4): 298-301.

[15] Brisman, J.L.; Song, J.K.; and Newell, D.W. (2006). Cerebral aneurysms. N Eng J Med 355: 928-939.

[16] White, J.B.; Ken, C.G.; Cloft, H.J.; and Kallmes, D.F. (2008). Coils in a nutshell: a review of coil physical properties. Am J Neuro Radiol 29: 1242-1246.

[17] Kotsiantis, S.B. (2007). Supervised machine learning: a review of classification techniques. Informatica 31: 249-268.

[18] Chen, H.H.; Pai, P.F.; Cho, Y.Z.; Lee, F.C.; and Fu, J.C. (2010). An improved support vector machines model in medical data analysis. Int J Math Model Numer Optim 1: 168-184.

[19] Yu, W.; Liu, T.; Valdez, R.; Gwinn, M.; and Knoury, M.J. (2010). Application of support vector machine modeling for prediction of common diseases: the case of diabetes and pre-diabetes. BMC Med Inform Decis Mak 22: 10-16.

[20] Zheng, R.Y. (2004). Biological applications of support vector machines. Brief Bioinform 5: 328-338.

[21] Sutton, C.D. (2005). Classification and regression trees, bagging and boosting. Handbook of statistics 24: 303-329.

[22] Math Works. Supervised learning (machine learning) workflow and algorithms [Online].1984-2011. Available from: http: //www.mathworks.com/ help/toolbox/stats/bsvjx5-1.html [2011, October 20]

[23] Soman, K.P.; Diwakar, S.; and Ajay Y. (2006). Insight into data mining: Theory and practice. New Delhi: Prentice-Hall of India Private Limited.

[24] Vapnik, V.; and Cortes, C. (1995). Support-vector networks. Mach Learn 20: 273-297.

[25] Gunn, S.R. (1998). Support vector machines for classification and regression. Technical report of Southampton university: 19-22.

[26] Chang, C.C.; and Lin, C.J. LIBSVM: a library for support vector machines. [Online]. 2011. Available from: http://www.csie.ntu.edu.tw/~cjlin/ libsvm.html [2011, Nov 5]

[27] Grant, M.; and Boyd, S. CVX: Matlab software for disciplined convex programming [Online]. 2012. Available from: http://www.cvxr.com/ cvx.html [2012, April 23]

[28] Mangiameli, P.; West, D.; and Rampal, R. (2004). Model selection for medical diagnosis decision support systems. Decision Support Systems 36: 247-259.

[29] Luo, S.T.; and Cheng, B.W. (2010). Diagnosing breast masses in digital mammography using feature selection and ensemble methods. J Med Syst Accessed 14 May 2010: PubMed PMID: 20703679.

[30] Morra, J.H.; Tu, Z.; Toga, A.W.; and Thompson, P.M. (2009). Lossless online ensemble learning (LOEL) and its application to subcortical segmentation. Med Image Comput Comput Assist Interv 12 (Pt 2): 432-440.

[31] Breiman, L. (1996). Bagging predictors. Mach Learn 24: 123-140.

[32] Alpaydin, E. (2004). Introduction to machine learning. Dietterich, T. eds. America. pp. 360.

[33] Schapire, R.E. (1990). The strength of weak learnability. Machine learning. 5(2): 197-227.

[34] Freund, Y.; and Schapire. (1997). A decision-theoretic generalization of on-line and application to Boosting. <u>J Comput Syst Sci</u> 55(1): 119-139.

[35] Ding, Y.H.; Dai, D.; Kadirvel, R.; Lewis, D.A.; Cloft, H.J.; and Kallmes, D.F. (2008). Relationship between aneurysm volume and histologic healing after coil embolization in elastase-induced aneurysms: a retrospective study. <u>Am J Neuro Radiol</u> 29: 98-101.

[36] Sluzewski, M.; Rooij, W.J.V.; Slob, M.J.; et al. (2004). Relation between aneurysm volume, packing, and compaction in 145 cerebral aneurysms treated with coils. <u>Radiology</u> 231: 653-658.

[37] Tamatani, S.; Ito, Y.; Abe, H.; Koike, T.; Takeuchi, S.; and Tanaka, R. (2002). Evaluation of the stability of aneurysm after embolization using detachable coils: correlation between stability of aneurysms and embolized volume of aneurysms. <u>Am J Neuro Radiol</u> 23: 762-767.

[38] Goddard, J.K.; Moran, C.J.; Cross, D.W.T.; and Derdeyn, C.P. (2005). Absent relationship between coil embolization ratio in small aneurysms treated with a single detachable coil and outcomes. <u>Am J Neuro Radiol</u> 26: 1916-1920.

[39] Slob, M.J.; Sluzewski, M.; and Rooij, W.J.V. (2005). The relation between packing and reopening in coiled intracranial aneurysm: a prospective study. <u>Neuroradiology</u> 47: 942-945.

[40] Piotin, M. (2007). Intracranial aneurysm: treatment with bare platinum coils - aneurysm packing, complex coils, and angiographic recurrence. <u>Radiology</u> 243: 500-508.

[41] Groden, C.; Laudan, J.; Gatchell, S.; and Zeumer, H. (2001). Three-dimensional pulsatile flow simulation before and after endovascular coil embolization of terminal cerebral aneurysm. <u>J Cereb Blood Flow Metab</u> 21: 1464-1471.

[42] Isaksen, J.G.; Bazilevs, Y.; Kvamsdal, T.; et al. (2008). Determination of wall tension in cerebral artery aneurysms by numerical simulation. <u>Stoke</u> 39: 3172-3178.

[43] Sforza, D.M.; Putman, C.M.; and Cebral, J.R. (2009). Hemodynamics of cerebral aneurysms. <u>Annu Rev Fluid Mech</u> 41: 91-107.

[44] Babiker, M.H.; Gonzalez, L.F.; Albuquerque, F.; Collins, D.; Elvikis, A.; and Frakes, D.H. (2010). Quantitative effects of coil packing density on cerebral aneurysm fluid dynamics: an in vitro steady flow study. Annals of Biomedical Engineering 38(7): 2293-2301.

[45] Gounergrits, L.; Thamsen, B.; Berthe, A.; et al. (2010). In vitro study of near-wall flow in a cerebral aneurysm model with and without coils. Am J Neuro Radiol May 20, 2010: 1-8.

[46] Mehra, M.; Hurley, M.C.; Gounis, M.J.; et al. (2011). The impact of coil shape design on angiographic occlusion, packing density and coil mass uniformity in aneurysm embolization: an in vitro study. J NeuroIntervent Surg 3: 131-136.

[47] Waranable, K.; Sugiu, K.; Tokunaga, K.; Sasahara, W.; Ono, S.; Date, I. (2007). Packing efficacy of hydrocoil embolic system: in vitro study using rupture aneurysm model. Neurosurg Rev 30: 127-130.

[48] Piotin, M.; Mandai, S.; Sugiu, K.; Gailloud, P.; and Rufenaht, D.A. (2000). Endovascular treatment of cerebral aneurysms: an in vitro study with detachable platinum coils and tricellulose acetate polymer. Am J Neuro Radiol 176: 235-239.

[49] Sugiu, K.; Tokunaga, K.; Mandai, S.; Martin, J.B.; Jean, B.; and Rufenacht, D.A. (2003). Spiral versus J-shaped coils for neurovascular embolization-an in-vitro study. Neuroradiology 45: 417-422.

[50] Piotin, M.; Mandai, S.; Murphy, K.J.; et al. (2000). Dense packing of cerebral aneurysms: an in vitro study with detachable platinum coils. Am J Neuro Radiol 21: 757-760.

[51] Cotin, S.; Duriez, C.; Lenoir, J.; Neumann, P.; Dawson, S. (2005). New approaches to catheter navigation for interventional radiology simulation. In: proceedings of MICCAI 3750: 534-542.

[52] Alderliesten, T. (2004). Simulation of minimally-invasive vascular interventions for training purposes. PhD dissertation, Utecht university.

[53] Dequidt, J.; Marchal, M.; Duriez, C.; Kerrien, E.; and Cotin, S. (2008). Interactive simulation of embolization coils: modeling and experimental validation. In: proceedings of MICCAI. 1-8.

[54] Dequidt, J.; Duriez, C.; Cotin, S.; and Kerrien, E. (2009). Toward interactive planning of coil embolization in brain aneurysm. In: proceedings of MICCAI: 377-385.

[55] Piotin, M.; Daghman, B.; Mounayer, C.; Spelle, L.; and Moret, J. (2006). Ellipsoid approximation versus 3D rotational angiography in the volumetric assessment of intracranial aneurysm. Am J Neuro Radiol 27: 839-842.

[56] Arlot, S.; and Celisse, A. (2010). A survey of cross-validation procedures for model selection. Statist Surv 4: 40-79.

[57] Orlando Regional Healthcare, Education and development. (2004). Overview of adult traumatic brain injuries [2008, January 16]

[58] Yoo, I.; Alafaireet, P.; Marinov, M.; Pena-Hernandez, K.; Gopidi, R.; Chang, J. F.; Hua, L. (2011). Data mining in healthcare and biomedicine: a survey of the literature. J Med Syst. Accessed 3 May 2011. PubMed PMID: 21537851.

[59] Chen, C.; Li, S.X.; Wang, S.M.; Liang, S.W. (2011). A support vector machine based pharmacodynamic prediction model for searching active fraction and ingredients of herbal medicine: Naodesheng prescription as an example. J Pharm Biomed Anal 56(2): 443-447.

[60] Thai, K.M.; Nquyen, T.Q.; Ngo, T.D.; Tran, T.D.; Huynh, T.N. (2012). A support vector machine classification model for Benzo[c]phenathridine analogues with Toposiomerase-I inhibitory activity. Molecules 17(4): 4560-4582.

[61] Mualla, F.; Pruemmer, M.; Hanh, D.; Hornegger, J.; (2012). Toward automatic detection of vessel stenoses in cerebral 3D DSA volumes. Phys Med Biol. 57(9): 2555-2573.

[62] Khoshgoftaar, T.M.; Van, H.J.; and Napolitano, A. (2011). Comparing boosting and bagging techniques with noisy and imbalanced data. IEEE T Syst Man Cy 41: 552-568.

[63] Zhang, P.; Zhang, Z.; Li, A.; Shi, Y. (2008). Global and local (glocal) bagging approach for classifying noisy dataset. Int J Softw Inform 2: 181-197.

VITAE

Personal Information

- ➤ **Name:** Mr. Wiwat Owasirikul
- ➤ **Home Address:** 119/37 Pruksa Ville, Kanchanapisek Road, Bang Kruai, Nonthaburi Thailand. 11130. E-mail: wiwat_o@hotmail.com, Tel: +668-998-59759.

Education

2000-2003   B.Sc. in Radiological Technology

Mahidol University, Nakorn Pathom, Thailand

2005-2007   M.Sc. in Radiological Technology

Mahidol University, Nakorn Pathom, Thailand

(under the University Development Commission (UDC) fellowship)

2008-2011   Ph.D. in Biomedical Engineering

Chulalongkorn University, Bangkok, Thailand

(under the University Development Commission (UDC) fellowship)

Field of Specialization

- ➤ Medical Imaging
- ➤ Medical Informatics

Scholarship

- ➤ The 90th Anniversary of Chulalongkorn University Fund (Ratchadaphiseksomphot Endowment Fund)
- ➤ Conference grant for Ph.D. student

International Conferences & Award

- ➤ Young Investigator Award from oral presentation in the 11th Asia-Oceania Congress of Medical Physics (AOCMP) in conjunction with the 6th Japan-Korea Joint Meeting on Medical Physics (JKMP), September 29-October 1, 2011 Fukuoka, Japan.
- ➤ Poster presentation in the 11th World Federation of Interventional and Therapeutic Neuroradiology (WFITN), November 8-10, 2011 Cape Town, South Africa.